International Journal of Control, Automation and Systems 15(5) (2017) 2329-2342
http://dx.doi.org/10.1007/s12555-016-0452-5
ISSN:1598-6446 eISSN:2005-4092
http://www.springer.com/12555

Robust Proportional-derivative Control on SO(3) with Disturbance Compensation for Quadrotor UAV

Andreas P. Sandiwan, Adha Cahyadi, and Samiadji Herdjunanto*

Abstract: This paper presents a control law that can counter both random disturbance and inertia matrix perturbation in quadrotor attitude stabilization. The control law consists of an ordinary proportional-derivative control and a disturbance compensation. The disturbance compensation is designed by creating a virtual force that always attracts the quadrotor's state variables back to the equilibrium point. Numerical simulations demonstrate that the control law can counter the effect of the disturbance and perturbation by reducing the upper bound of solution and reducing the vibration effectively.

Keywords: Disturbance compensation, proportional-derivative (PD) control, quadrotor, rotation in SO(3).

1. INTRODUCTION

Unmanned Aerial Vehicle (UAV) is a flying machine that can be remotely controlled or fly autonomously. UAVs are popularly used for commercial, military, and academic purposes [1]. Currently, UAVs' usages in commercial and academic environment increase as their prices get cheaper. Quadrotor is an appealing UAV type because it has simple mechanical structure [2]. Instead of using swashplate like common helicopter, quadrotor controls rotational speed of its four rotors to manipulate its attitude. This yields the need of attitude control algorithm that controls the rotors' rotational speed [3].

In order to control the attitude of a quadrotor, one needs to represent the attitude properly. There are three approaches to attitude control. The first approach controls roll, pitch, and yaw (RPY) angles separately, which is called separate RPY control as shown in [4]. The second method uses quaternions as attitude representation. Although quaternions do not have singularities, a single attitude may be represented by two antipodal points on the three-sphere [5]. The third approach considers quadrotor's kinematics equation in SO(3) group. The separate RPY control, despite its popularity, neglects the manifold structure of rotation and cannot avoid singularity in the rotation matrix. In the case of RPY attitude representation, singularity occurs when the pitch angle equals 90° [6]. The third approach has an advantage over the other two, that is its ability to avoid singularity of roll, pitch, and yaw angle, and quaternions' double covering problem [5]. Several prior works that used this approach were Yu [4], Yu [6], Lee [5, 7, 9], and Fernando [10].

Quadrotor has wide applications that set new demands and expectations for quadrotor to operate in harsh environments [11]. This requires the quadrotor to be able to handle disturbance, which is a challenging problem in quadrotor control [12]. There are many factors that contribute to disturbance, such as wind, blade flapping, and unmodeled motor and propeller dynamics. In addition to disturbance, there are always parametric uncertainties such as perturbation or uncertainties of inertia matrix [13].

Some works approached the disturbance problem by detailed modelling of aerodynamics and wind effects on quadrotor to estimate the disturbance, like those conducted by Sydney [14], Tran [15], and Huang [16]. Sydney created compensation term in control law by estimating wind effects on the quadrotor propeller. Tran studied the interaction between propeller and wind, but did not make any compensation. Huang [16] created disturbance compensation for aggressively-maneuvering quadrotor by considering blade flapping. Those works demonstrated good results, but required a detailed model regarding the effects of wind and detailed aerodynamics.

Another important challenge to address is inertia matrix perturbation, which is a case of parametric uncertainties. Sheng [13] designed an adaptive attitude tracking control for unmanned helicopter using adaptive law. He successfully demonstrated the good performance of his control

Manuscript received August 22, 2016; revised December 20, 2016; accepted January 17, 2017. Recommended by Associate Editor Hyo-Sung Ahn under the direction of Editor Myo Taeg Lim. The authors would like to thank the Faculty of Engineering, Universitas Gadjah Mada, for providing PPI grant to support this research.

Andreas P. Sandiwan is a bachelor graduate of Department of Electrical Engineering and Information Technology, Faculty of Engineering, Universitas Gadjah Mada, Jl. Grafika 2 Yogyakarta 55281, Indonesia (e-mail: aprasetyantosandiwan@gmail.com). Adha Cahyadi and Samiadji Herdjunanto are with Department of Electrical Engineering and Information Technology, Faculty of Engineering, Universitas Gadjah Mada, Jl. Grafika 2 Yogyakarta 55281, Indonesia (e-mails: {masimam, samiadji}@jteti.gadjahmada.edu).
* Corresponding author.

law via numerical simulation. Goodarzi [8] designed an algorithm that can control a quadrotor UAV transporting a payload connected via flexible cable.

A prior work in robust adaptive attitude tracking using SO(3) representation has been made by Lee in [9], which is an extension from Fernando's work [10]. They approached the inertia matrix perturbation problem by using adaptive law. The disturbance was handled by a compensation term that has a form similar to a signum function.

The objective of this research is to design a disturbance compensation method and to investigate the effectiveness of the disturbance compensation in countering disturbance and inertia matrix perturbation. Compared to the works made by [9] and [10], this paper aims at stabilization control, which is quite different from tracking control. Because of different error functions and design and analysis concept, the compensation term in those works is not directly applicable to stabilization case; thus, it is modified in this paper.

Moreover, in this paper, the disturbance is generalized as a torque vector. This approach has an advantage that it can cover general type of disturbance, such as wind, blade flapping, and motor and propeller nonidealities. It can also counter inertia matrix perturbation. This paper demonstrates that for stabilization case, no adaptive law is required to counter the inertia matrix perturbation. In addition, no detailed model or estimation for wind or aerodynamic effects is required to design disturbance compensation.

The remainder of this paper is arranged in 5 sections. Rotation in SO(3) is explained in Section 2. This is continued by Section 3 that explains quadrotor model in SO(3). Section 4 describes proportional-derivative (PD) control without and with disturbance and compensation. Next, the numerical simulation and analysis are presented in Section 5. Finally, this paper is concluded in Section 6.

2. MATHEMATICS OF ROTATION IN SO(3)

In this section we address the necessary mathematics for operation in SO(3) group, mainly based on [4], [17], and [18]. According to Euler's theorem, any 3-dimensional rotation of rigid body can be represented by a rotation of a given axis by an angle. This is the primary feature of the SO(3) representation. This feature distinguishes the SO(3) representation from its more popular counterpart, namely the roll, pitch, yaw (RPY) representation. The RPY representation uses composition of three consecutive rotations, while SO(3) representation only uses single axis in $\Re^3$.

Suppose that $\boldsymbol{\omega} \in \Re^3$ is a unit vector specifying the rotation axis of a rigid body, and $\varphi \in \Re$ is rotation angle in radians. The position of a point at the rigid body as a function of time is denoted by $\mathbf{q}(t)$. Rotation at constant $\boldsymbol{\omega}$ yields the point's translational velocity as

$$\dot{\mathbf{q}}(t) = \boldsymbol{\omega} \times \mathbf{q}(t) = \hat{\boldsymbol{\omega}}\mathbf{q}(t). \tag{1}$$

The hat notation maps a vector in $\Re^3$ to a skew-symmetric matrix,

$$\hat{\boldsymbol{\omega}} = \begin{bmatrix} 0 & -\omega_3 & \omega_2 \\ \omega_3 & 0 & -\omega_1 \\ -\omega_2 & \omega_1 & 0 \end{bmatrix}. \tag{2}$$

We denote the inverse mapping from $\hat{\boldsymbol{\omega}}$ to $\boldsymbol{\omega}$ as $\vee$ (vee), such that $\hat{\boldsymbol{\omega}}^{\vee} = \boldsymbol{\omega}$. All such matrices form a vector space named so(3),

$$\mathrm{so}(3) = \left\{ \mathbf{S} \in \Re^{3\times 3} | \mathbf{S}^T = -\mathbf{S} \right\}. \tag{3}$$

Rotation matrix $\mathbf{R}$ belongs to SO(3) group, defined as

$$\mathrm{SO}(3) = \left\{ \mathbf{R} \in \Re^3 | \mathbf{R}^{-1} = \mathbf{R}^T, \det(\mathbf{R}) = +1 \right\}. \tag{4}$$

The SO(3) group, which is a Lie group, actually means "Special Orthogonal-3" group, which means a group of 3-by-3 orthogonal matrices. Orthogonal matrices are characterized by $\mathbf{R}^{-1} = \mathbf{R}^T$. The group has the name special because the matrix determinant is always +1. On the other hand, the so(3) group, which contains skew-symmetric matrices, is the Lie algebra of SO(3). Further explanation can be found in [17].

We map matrices from so(3) to SO(3) using exponential map as

$$\mathbf{R} = \exp(\hat{\boldsymbol{\omega}}\varphi) = \mathbf{I} + \varphi\hat{\boldsymbol{\omega}} + \frac{1}{2!}(\varphi\hat{\boldsymbol{\omega}})^2 + \frac{1}{3!}(\varphi\hat{\boldsymbol{\omega}})^3 + \cdots. \tag{5}$$

Equation (5) is commonly written as Rodrigues' formula:

$$\exp(\hat{\boldsymbol{\omega}}\varphi) = \mathbf{I} + \frac{\hat{\boldsymbol{\omega}}}{\|\boldsymbol{\omega}\|}\sin(\|\boldsymbol{\omega}\|\varphi) + \frac{\hat{\boldsymbol{\omega}}^2}{\|\boldsymbol{\omega}\|^2}(1-\cos(\|\boldsymbol{\omega}\|\varphi)). \tag{6}$$

For $\|\boldsymbol{\omega}\| = 1$, (6) becomes

$$\exp(\hat{\boldsymbol{\omega}}\varphi) = \mathbf{I} + \hat{\boldsymbol{\omega}}\sin(\varphi) + \hat{\boldsymbol{\omega}}^2(1-\cos(\varphi)). \tag{7}$$

Inverse mapping from SO(3) to so(3) is done by the logarithmic map, which is defined as

$$\log(\mathbf{R}) = \frac{\varphi}{2\sin\varphi}\left(\mathbf{R} - \mathbf{R}^T\right), \tag{8}$$

where φ is $\arccos\left(\frac{tr(\mathbf{R})-1}{2}\right)$ and $|\varphi| < \pi$. Moreover, if $\mathbf{R} = \mathbf{I}$, $\boldsymbol{\omega}$ can be chosen arbitrarily. The result of equation (8) is still in skew-symmetric matrix of so(3) group. We can write it in terms of $\Re^3$ by using the $\vee$ operator as

$$\boldsymbol{\zeta} = \log(\mathbf{R})^{\vee}. \tag{9}$$

3. QUADROTOR UAV MODEL

This section explains quadrotor model based on the works of Ataka [19] and [20]. The quadrotor model is shown in Fig. 1. It also shows quadrotor's position in the inertial frame, which is denoted by vector $\mathbf{r} = \begin{bmatrix} x & y & z \end{bmatrix}$. In Fig. 1, the quadrotor's attitude is described using roll (ϕ), pitch (θ), and yaw (ψ) angle, written as $\mathbf{\Psi} = \begin{bmatrix} \phi & \theta & \psi \end{bmatrix}^T$. The angular velocity is described in body frame axes, denoted as $\mathbf{\Omega}_b = \begin{bmatrix} p & q & r \end{bmatrix}^T$. Note that the non-unit vector $\mathbf{\Omega}_b$ denotes the angular velocity in body frame. Meanwhile, the vector $\boldsymbol{\omega}$ in the previous section denotes the unit vector specifying the rotation axis. The relationship between them is $\mathbf{\Omega}_b = \varphi\boldsymbol{\omega}$, where φ is described in (8).

The inertia matrix of the quadrotor is as follows:

$$\mathbf{J} = \begin{bmatrix} J_{xx} & J_{xy} & J_{xz} \\ J_{xy} & J_{yy} & J_{yz} \\ J_{xz} & J_{yz} & J_{zz} \end{bmatrix}, \tag{10}$$

where the indices x, y, and z in (10) denote x-,y-, and z-axis in the body frame, respectively. For simplicity, we assume that the quadrotor is symmetric to its x- and y-axis as in [21]. This eliminates the axis coupling in quadrotor system. Therefore, according to [22], the off-diagonal elements of the inertia matrix are zero, and equation (10) can be written as

$$\mathbf{J} = \begin{bmatrix} J_{xx} & 0 & 0 \\ 0 & J_{yy} & 0 \\ 0 & 0 & J_{zz} \end{bmatrix}. \tag{11}$$

Quadrotor's system inputs are the squared angular speeds of its four rotors, denoted by $\mathbf{w} = \begin{bmatrix} w_1^2 & w_2^2 & w_3^2 & w_4^2 \end{bmatrix}^T$. The rotors generate the torques $\boldsymbol{\tau} = \begin{bmatrix} \tau_x & \tau_y & \tau_z \end{bmatrix}$ and thrust T. The torques and thrust

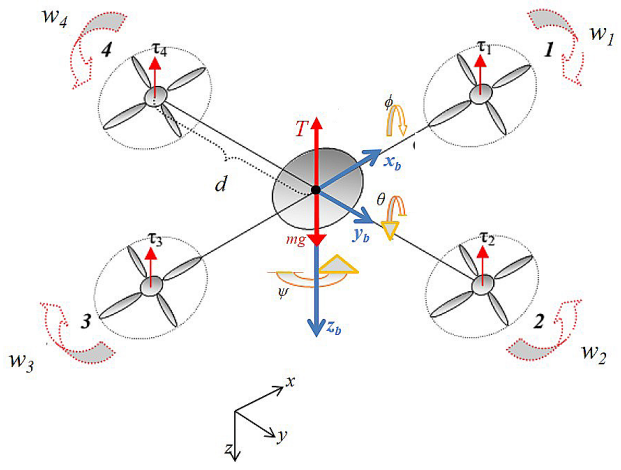

Fig. 1. Quadrotor model.

are generated by manipulating the angular speeds as

$$\tau_x = db\left(w_4^2 - w_2^2\right), \tag{12}$$

$$\tau_y = db\left(w_1^2 - w_3^2\right), \tag{13}$$

$$\tau_z = k\left(w_1^2 - w_2^2 + w_3^2 - w_4^2\right), \tag{14}$$

and

$$T = k\left(w_1^2 + w_2^2 + w_3^2 + w_4^2\right). \tag{15}$$

In equation (12) to (15), d, b, k are respectively the length of the quadrotor's arm, propeller thrust coefficient, and propeller torque coefficient.

The quadrotor's dynamics is defined by Euler equation, i.e.,

$$\tau = \mathbf{J}\dot{\mathbf{\Omega}}_b + \mathbf{\Omega}_b \times \mathbf{J}\mathbf{\Omega}_b, \tag{16}$$

which can be rewritten as

$$\dot{\mathbf{\Omega}}_b = -\mathbf{J}^{-1}(\mathbf{\Omega}_b \times \mathbf{J}\mathbf{\Omega}_b) + \mathbf{J}^{-1}\tau, \tag{17}$$

and quadrotor kinematics is defined by

$$\dot{\mathbf{R}} = \mathbf{R}\hat{\mathbf{\Omega}}_b. \tag{18}$$

We can write the differential equation (18) in terms of the angle $\boldsymbol{\zeta}$ as

$$\dot{\boldsymbol{\zeta}} = \left(\mathbf{I} + \frac{1}{2}\hat{\boldsymbol{\zeta}} + \left(1 - \alpha(\|\boldsymbol{\zeta}\|)\frac{\hat{\boldsymbol{\zeta}}}{\|\boldsymbol{\zeta}\|}\right)\right)\mathbf{\Omega}_b, \tag{19}$$

where $\alpha(\|\boldsymbol{\zeta}\|) = \frac{\zeta}{2}\cot\frac{\zeta}{2}$ [17]. With equation (17) and (19), the second order system of quadrotor UAV in SO(3) is defined as

$$\begin{cases} \dot{\boldsymbol{\zeta}} = \left(\mathbf{I} + \frac{1}{2}\hat{\boldsymbol{\zeta}} + \left(1 - \alpha(\|\boldsymbol{\zeta}\|)\frac{\hat{\boldsymbol{\zeta}}}{\|\boldsymbol{\zeta}\|}\right)\right)\mathbf{\Omega}_b, \\ \dot{\mathbf{\Omega}}_b = -\mathbf{J}^{-1}(\mathbf{\Omega}_b \times \mathbf{J}\mathbf{\Omega}_b) + \mathbf{J}^{-1}\tau. \end{cases} \tag{20}$$

4. ROBUST PROPORTIONAL-DERIVATIVE CONTROL FOR QUADROTOR IN SO(3)

This section is divided into three parts. The first part explains proportional-derivative (PD) control in nominal condition (without disturbance and perturbation). The second part addresses the design and analysis of disturbance compensation. The third part deals with the inertia matrix perturbation. The fourth part concludes this section by writing down the control algorithm under disturbance and inertia matrix perturbation.

4.1. PD Control in nominal condition

Stabilization of quadrotor system can be achieved using PD control already developed by [17].

Theorem 1: (PD plus feedforward control on SO(3)) The quadrotor system in (20) can be asymptotically stabilized by the following PD control law:

$$\boldsymbol{\tau} = \boldsymbol{\Omega}_b \times \mathbf{J}\boldsymbol{\Omega}_b - \mathbf{K}_p\boldsymbol{\zeta} - \mathbf{K}_d\boldsymbol{\Omega}_b, \tag{21}$$

where $\mathbf{K}_p$ and $\mathbf{K}_d$ are symmetric, positive definite gain matrices and $\boldsymbol{\zeta} = \log(\mathbf{R})^\vee$.

Proof: The closed-loop system satisfies

$$\begin{aligned}\dot{\boldsymbol{\zeta}} &= \sum_{n=0}^{\infty} \frac{(-1)^n \mathrm{B}_n}{n!} \left(\mathrm{ad}^n_{\boldsymbol{\zeta}}\left(\hat{\boldsymbol{\Omega}}_b\right)\right)^\vee = \left(\beta_{\hat{\boldsymbol{\zeta}}}\hat{\boldsymbol{\Omega}}_b\right)^\vee, \\ \dot{\boldsymbol{\Omega}}_b &= -\mathbf{J}^{-1}\mathbf{K}_p\boldsymbol{\zeta} - \mathbf{J}^{-1}\mathbf{K}_d\boldsymbol{\Omega}_b,\end{aligned} \tag{22}$$

where $\{\mathrm{B}_n\}$ denotes Bernoulli numbers [17]. Bernoulli numbers are a sequence of a signed rational numbers that can be defined as the exponential generating function:

$$\frac{x}{e^x - 1} = \sum_{n=0}^{\infty} \frac{B_n x^n}{n!}. \tag{23}$$

The first few Bernoulli numbers from $n = 0$ to 8 are 1, -1/2, 1/6, -1/30, 1/42, and -1/30, respectively. Meanwhile, the ad operator, which works on so(3) group, is defined as

$$\mathrm{ad}^n_{\hat{\boldsymbol{\zeta}}}\left(\hat{\boldsymbol{\Omega}}_b\right) = \left(\hat{\boldsymbol{\zeta}}\hat{\boldsymbol{\Omega}}_b - \hat{\boldsymbol{\Omega}}_b\hat{\boldsymbol{\zeta}}\right)^n. \tag{24}$$

With the $\vee$ operator, equation (24) becomes

$$\left(\mathrm{ad}^n_{\hat{\boldsymbol{\zeta}}}\left(\hat{\boldsymbol{\Omega}}_b\right)\right)^\vee = \hat{\boldsymbol{\zeta}}^n\boldsymbol{\Omega}_b. \tag{25}$$

Meanwhile, $\beta_{\hat{\boldsymbol{\zeta}}}$ is

$$\beta_{\hat{\boldsymbol{\zeta}}} = \sum_{n=0}^{\infty} \frac{(-1)^n \mathrm{B}_n}{n!} \mathrm{ad}^n_{\hat{\boldsymbol{\zeta}}}. \tag{26}$$

As a note, the kinematics equation in (22) is obtained from

$$\begin{aligned}\dot{\boldsymbol{\zeta}} &= \sum_{n=0}^{\infty} \frac{(-1)^n \mathrm{B}_n}{n!} \left(\mathrm{ad}^n_{\boldsymbol{\zeta}}\left(\hat{\boldsymbol{\Omega}}_b\right)\right)^\vee \\ &= \sum_{n=0}^{\infty} \left[\frac{(-1)^n \mathrm{B}_n}{n!} \left(\mathrm{ad}^n_{\boldsymbol{\zeta}}\left(\hat{\boldsymbol{\Omega}}_b\right)\right)\right]^\vee \\ &= \left[\sum_{n=0}^{\infty} \frac{(-1)^n \mathrm{B}_n}{n!} \left(\mathrm{ad}^n_{\boldsymbol{\zeta}}\left(\hat{\boldsymbol{\Omega}}_b\right)\right)\right]^\vee \\ &= \left(\beta_{\hat{\boldsymbol{\zeta}}}\hat{\boldsymbol{\Omega}}_b\right)^\vee.\end{aligned} \tag{27}$$

The step from the first line to the third line of (27) can be made because $((-1)^n \mathrm{B}_n)/n!$ is a scalar. Further explanation about Bernoulli numbers, the ad operator, and $\beta_{\hat{\boldsymbol{\zeta}}}$ can be seen at [17].

The following Lyapunov function can be used to prove the stability of (20) under control law (21):

$$W = \frac{1}{2}\left\langle \begin{bmatrix}\boldsymbol{\zeta} \\ \boldsymbol{\Omega}_b\end{bmatrix}, \begin{bmatrix}\mathbf{I}_{3\times3} & \varepsilon\mathbf{I}_{3\times3} \\ \varepsilon\mathbf{I}_{3\times3} & \mathbf{K}_p^{-1}\mathbf{J}\end{bmatrix}\begin{bmatrix}\boldsymbol{\zeta} \\ \boldsymbol{\Omega}_b\end{bmatrix}\right\rangle, \tag{28}$$

where $\mathbf{I}_{3\times3}$ is a 3 by 3 identity matrix. This can be simplified to

$$W = \frac{1}{2}\boldsymbol{\xi}^T\mathbf{P}_\varepsilon\boldsymbol{\xi}, \tag{29}$$

where

$$\boldsymbol{\xi} = \begin{bmatrix}\boldsymbol{\zeta} \\ \boldsymbol{\Omega}_b\end{bmatrix}, \tag{30}$$

and

$$\mathbf{P}_\varepsilon = \begin{bmatrix}\mathbf{I}_{3\times3} & \varepsilon\mathbf{I}_{3\times3} \\ \varepsilon\mathbf{I}_{3\times3} & \mathbf{K}_p^{-1}\mathbf{J}\end{bmatrix}. \tag{31}$$

The time derivative of (28) alongside (22) is given as

$$\begin{aligned}\dot{W} &= \left\langle \boldsymbol{\zeta}, \dot{\boldsymbol{\zeta}} \right\rangle + \left\langle \boldsymbol{\Omega}_b, \mathbf{K}_p^{-1}\mathbf{J}\dot{\boldsymbol{\Omega}}_b \right\rangle \\ &\quad \varepsilon\left\langle (\beta_{\hat{\boldsymbol{\zeta}}}\hat{\boldsymbol{\Omega}}_b)^\vee, \boldsymbol{\Omega}_b \right\rangle + \varepsilon\left\langle \boldsymbol{\zeta}, \dot{\boldsymbol{\Omega}}_b \right\rangle \\ &\leq \left\langle \boldsymbol{\zeta}, \dot{\boldsymbol{\zeta}} \right\rangle + \left\langle \boldsymbol{\Omega}_b, \mathbf{K}_p^{-1}\mathbf{J}\dot{\boldsymbol{\Omega}}_b \right\rangle \\ &\quad + \varepsilon\left\langle \boldsymbol{\Omega}_b, \boldsymbol{\Omega}_b \right\rangle + \varepsilon\left\langle \boldsymbol{\zeta}, \dot{\boldsymbol{\Omega}}_b \right\rangle \\ &\leq \left\langle \boldsymbol{\zeta}, \boldsymbol{\Omega}_b \right\rangle + \left\langle \boldsymbol{\Omega}_b, \mathbf{K}_p^{-1}\mathbf{J}\dot{\boldsymbol{\Omega}}_b \right\rangle \\ &\quad + \varepsilon\left\langle \boldsymbol{\Omega}_b, \boldsymbol{\Omega}_b \right\rangle + \varepsilon\left\langle \boldsymbol{\zeta}, \dot{\boldsymbol{\Omega}}_b \right\rangle \\ &= \left\langle \boldsymbol{\zeta}, \boldsymbol{\Omega}_b \right\rangle \\ &\quad + \left\langle \boldsymbol{\Omega}_b, \mathbf{K}_p^{-1}\mathbf{J}\left(-\mathbf{J}^{-1}\mathbf{K}_p\boldsymbol{\zeta} - \mathbf{J}^{-1}\mathbf{K}_d\boldsymbol{\Omega}_b\right) \right\rangle \\ &\quad + \varepsilon\left\langle \boldsymbol{\Omega}_b, \boldsymbol{\Omega}_b \right\rangle \\ &\quad + \varepsilon\left\langle \boldsymbol{\zeta}, -\mathbf{J}^{-1}\mathbf{K}_p\boldsymbol{\zeta} - \mathbf{J}^{-1}\mathbf{K}_d\boldsymbol{\Omega}_b \right\rangle \\ &\leq -\left\langle \boldsymbol{\Omega}_b, \mathbf{K}_p^{-1}\mathbf{K}_d\boldsymbol{\Omega}_b \right\rangle + \varepsilon\left\langle \boldsymbol{\Omega}_b, \boldsymbol{\Omega}_b \right\rangle \\ &\quad - \varepsilon\left\langle \boldsymbol{\zeta}, \mathbf{J}^{-1}\mathbf{K}_p\boldsymbol{\zeta} \right\rangle - \varepsilon\left\langle \boldsymbol{\zeta}, \mathbf{J}^{-1}\mathbf{K}_d\boldsymbol{\Omega}_b \right\rangle.\end{aligned} \tag{32}$$

The simplification of $\left\langle \boldsymbol{\zeta}, \dot{\boldsymbol{\zeta}} \right\rangle$ in (32) uses the fact that

$$\left\langle \boldsymbol{\zeta}, \dot{\boldsymbol{\zeta}} \right\rangle = \left\langle \boldsymbol{\zeta}, \boldsymbol{\Omega}_b \right\rangle, \tag{33}$$

as used in [17]. The reason for this is beyond the scope of this paper, and readers should consult [17] for details. In addition, we also use the following upper bound stated in [17] as

$$\left\langle (\beta_{\hat{\boldsymbol{\zeta}}}\hat{\boldsymbol{\Omega}}_b)^\vee, \boldsymbol{\Omega}_b \right\rangle \leq \left\langle \boldsymbol{\Omega}_b, \boldsymbol{\Omega}_b \right\rangle. \tag{34}$$

For simplicity, inequality (32) can be written in quadratic form, i.e.,

$$\dot{W} \leq -\boldsymbol{\xi}^T\mathbf{Q}_\varepsilon\boldsymbol{\xi}, \tag{35}$$

where

$$\mathbf{Q}_\varepsilon = \begin{bmatrix}\varepsilon\mathbf{J}^{-1}\mathbf{K}_p & \frac{\varepsilon}{2}\mathbf{J}^{-1}\mathbf{K}_d \\ \frac{\varepsilon}{2}\mathbf{J}^{-1}\mathbf{K}_d & \mathbf{K}_p^{-1}\mathbf{K}_d - \varepsilon\mathbf{I}_{3\times3}\end{bmatrix}. \tag{36}$$

The matrix $\mathbf{Q}_\varepsilon$ is positive definite. However, it is questioned for what values of ε, $\mathbf{P}_\varepsilon$ and $\mathbf{Q}_\varepsilon$ can be guaranteed

to be positive definite. It is easy to verify that $\mathbf{Q}_\varepsilon$ is positive definite for small ε. However, the upper bound for ε that makes $\mathbf{P}_\varepsilon$ and $\mathbf{Q}_\varepsilon$ positive definite is interesting to discuss. To simplify the discussion, let us assume that $\mathbf{K}_p$ and $\mathbf{K}_d$ are diagonal, i.e.,

$$\mathbf{K}_p = \begin{bmatrix} k_{p1} & 0 & 0 \\ 0 & k_{p2} & 0 \\ 0 & 0 & k_{p3} \end{bmatrix},$$
$$\mathbf{K}_d = \begin{bmatrix} k_{d1} & 0 & 0 \\ 0 & k_{d2} & 0 \\ 0 & 0 & k_{d3} \end{bmatrix}. \tag{37}$$

By checking the leading principal minors of $\mathbf{Q}_\varepsilon$, it is straightforward to verify that the condition for ε can be written as

$$\varepsilon < \min\left\{ \frac{k_{d1}}{k_{p1}\chi_1}, \frac{k_{d2}}{k_{p2}\chi_2}, \frac{k_{d3}}{k_{p3}\chi_3}, \sqrt{\frac{J_{xx}}{k_{p1}}}, \sqrt{\frac{J_{yy}}{k_{p2}}}, \sqrt{\frac{J_{zz}}{k_{p3}}} \right\}, \tag{38}$$

where

$$\chi_1 = 1 + \frac{k_{d1}^2}{4J_{xx}^2 k_{p1}},$$
$$\chi_2 = 1 + \frac{k_{d2}^2}{4J_{yy}^2 k_{p2}},$$
$$\chi_3 = 1 + \frac{k_{d3}^2}{4J_{zz}^2 k_{p3}}. \tag{39}$$

If ε fulfills the condition in (38), $\mathbf{P}_\varepsilon$ and $\mathbf{Q}_\varepsilon$ are guaranteed to be positive definite, making the closed-loop system asymptotically stable. The analysis related to the value of ε is conducted in Section 5, where the numerical values are available. □

Remark 1: (Error Term) Usually, PD control uses proportional and derivative error term. For example, if we wanted to control a variable y to match the constant set point y_d with PD control, the control law v would be

$$\begin{aligned} v &= -k_p(y - y_d) - k_d \frac{d(y - y_d)}{dt} \\ &= -k_p(y - y_d) - k_d \dot{y}, \end{aligned} \tag{40}$$

where k_p and k_d are proportional and derivative constant, respectively. In this particular example, the proportional error term is $e_p = y - y_d$, while the derivative error term is $e_d = \frac{d}{dt}(y - y_d) = \dot{y}$. With this in mind, equation (21) should be written as

$$\boldsymbol{\tau} = \boldsymbol{\Omega}_b \times \mathbf{J}\boldsymbol{\Omega}_b - \mathbf{K}_p(\boldsymbol{\zeta} - \boldsymbol{\zeta}_d) - \mathbf{K}_d\boldsymbol{\Omega}_b, \tag{41}$$

where $\boldsymbol{\zeta}_d$ is the constant set point of $\boldsymbol{\zeta}$. However, in this paper, the constant set point is $\boldsymbol{\zeta}_d = \mathbf{0}$ because we only consider stabilization. Therefore, we are left with just $\boldsymbol{\zeta}$ (and there is no $\boldsymbol{\zeta}_d$) in equation (21).

Remark 2: (Upper bound for ε) From (38) the upper bound for ε can be estimated roughly from the inertia matrix. The larger the diagonal components of the inertia matrix, the larger upper bound can be applied.

Remark 3: (Feedforward compensation) The word "feedforward" in Theorem 1 refers to the cross-term $\boldsymbol{\Omega}_b \times \mathbf{J}\boldsymbol{\Omega}_b$ in (21). The complete terminology is actually "feedforward compensation". This cross-term is introduced in (21) to cancel (or compensate) the cross-term $\boldsymbol{\Omega}_b \times \mathbf{J}\boldsymbol{\Omega}_b$ in (16). As a result, the cross-term vanishes in the closed-loop system's dynamics equation (second line of (22)).

4.2. PD control under disturbance

4.2.1 Design of disturbance compensation

Disturbance is encountered in almost any real quadrotor flight. Mostly, the disturbance is caused by aerodynamic effects and wind. Here we model the disturbance by the variable $\mathbf{g}$.

First, let us design the compensation term. Consider the vector space of quadrotor state variables, i.e. $\boldsymbol{\zeta}$ and $\boldsymbol{\Omega}_b$ shown in Fig. 2. Point $(\boldsymbol{\zeta}(t), \boldsymbol{\Omega}_b(t))$ shows an arbitrary position of state variable vectors at a point of time in quadrotor motion. By looking at equation (21), we know that the proportional and derivative term attract the state variables (nonzero $\boldsymbol{\zeta}$ and $\boldsymbol{\Omega}_b$) to the origin (where $\boldsymbol{\zeta}$ and $\boldsymbol{\Omega}_b$ equal zero). If there is a disturbance, then the system is pushed away from the origin. The proportional and derivative term may be able to counter the disturbance, but their ability is limited. This can be illustrated by considering the constant disturbance case. If a constant disturbance is present, the system might reach a steady condition where $\boldsymbol{\Omega}_b = \mathbf{0}$. However, in that condition, the proportional term must compensate the disturbance. This makes the angle $\boldsymbol{\zeta}$ deviate from the set point. If the disturbance is random, the angular velocity will be nonzero, making the derivative term also responsible for compensating the disturbance. To solve this problem, we need a disturbance compensation term to aid the PD controller in handling the distur-

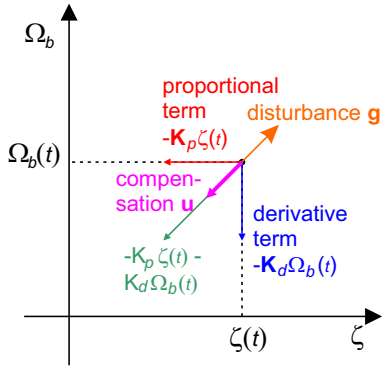

Fig. 2. Illustration of quadrotor's state variable vector space. The green dashed arrow is the compensation, while the orange one is the disturbance.

bance.

In this research, we compensate the disturbance by introducing a virtual force that always attracts the state variables back to the origin. This is an alternative to compensation design by estimating the disturbance. We use a mechanism that is also used in [9] and [10]. This mechanism only uses the upper bound of the disturbance magnitude to determine the magnitude of the compensation. The force is set to be directed to the origin. Therefore, the direction of the compensation $\mathbf{u}$, which is denoted by the unit vector $\mathbf{u}/\|\mathbf{u}\|$, is

$$\begin{aligned}\frac{\mathbf{u}}{\|\mathbf{u}\|} &= -\frac{\mathbf{K}_p\boldsymbol{\zeta}+\mathbf{K}_p\boldsymbol{\Omega}_b}{\|\mathbf{K}_p\boldsymbol{\zeta}+\mathbf{K}_p\boldsymbol{\Omega}_b\|}\\ &= -\mathrm{sgn}\left(\mathbf{K}_p\boldsymbol{\zeta}+\mathbf{K}_p\boldsymbol{\Omega}_b\right).\end{aligned} \tag{42}$$

The reason for multiplying $\mathbf{K}_p$ by $\boldsymbol{\zeta}$ and $\boldsymbol{\Omega}_b$ will be clear in the Lyapunov analysis. The matrix $\mathbf{K}_p$ is multiplied by $\boldsymbol{\zeta}$ and $\boldsymbol{\Omega}_b$ to give equal weighting on both of them. Because the magnitude of $\mathbf{u}$ should be bounded by the upper bound of disturbance magnitude, namely δ, the compensation $\mathbf{u}$ can be written as

$$\begin{aligned}\mathbf{u} &= -\frac{\delta\left(\mathbf{K}_p\boldsymbol{\zeta}+\mathbf{K}_p\boldsymbol{\Omega}_b\right)}{\|\mathbf{K}_p\boldsymbol{\zeta}+\mathbf{K}_p\boldsymbol{\Omega}_b\|}\\ &= -\delta\,\mathrm{sgn}\left(\mathbf{K}_p\boldsymbol{\zeta}+\mathbf{K}_p\boldsymbol{\Omega}_b\right).\end{aligned} \tag{43}$$

This signum function, however, suffers discontinuity at $\mathbf{K}_p\boldsymbol{\zeta}+\mathbf{K}_p\boldsymbol{\Omega}_b$ equals $\mathbf{0}$. This discontinuity can cause chattering (as shown further in Section 5). Therefore, we add a small scalar number κ to the denominator in the right-hand side of equation (43), so that it becomes

$$\mathbf{u} = -\frac{\delta\left(\mathbf{K}_p\boldsymbol{\zeta}+\mathbf{K}_p\boldsymbol{\Omega}_b\right)}{\|\mathbf{K}_p\boldsymbol{\zeta}+\mathbf{K}_p\boldsymbol{\Omega}_b\|+\kappa}. \tag{44}$$

Let us compare the compensation (44) with the compensation designed by Lee [9] and Fernando [10]. First, it has to be noted that they worked on tracking control, so they used different error functions. They used three error functions (all in vector form), i.e. attitude error vector $\mathbf{e}_R$, angular velocity error vector $\mathbf{e}_\Omega$, and augmented error vector $\mathbf{e}_A = \mathbf{e}_\Omega + c\mathbf{e}_R$, where c is a positive constant. The compensation they designed was

$$\mathbf{u}_{\text{Lee,Fernando}} = -\frac{\delta^2\mathbf{e}_A}{\delta\|\mathbf{e}_A\|+\varepsilon}, \tag{45}$$

where ε is a small positive number like κ in (43). The attitude error vector $\mathbf{e}_R$ is comparable to proportional error term $\boldsymbol{\zeta}-\boldsymbol{\zeta}_d = \boldsymbol{\zeta}$ in (21), and the angular velocity error vector $\mathbf{e}_\Omega$ is comparable to $\boldsymbol{\Omega}_b$ in (21). The augmented error vector $\mathbf{e}_A$ is comparable to $(\mathbf{K}_p\boldsymbol{\zeta}+\mathbf{K}_p\boldsymbol{\Omega}_b)$. The form of the compensation (44) itself is similar to (45).

4.2.2 Lyapunov analysis of the disturbance compensation

To prove the stability of the system with the presence of the compensation $\mathbf{u}$, we modify the Lyapunov function in (28) into

$$\begin{aligned}W &= \frac{1}{2}\left\langle\begin{bmatrix}\boldsymbol{\zeta}\\ \boldsymbol{\Omega}_b\end{bmatrix},\begin{bmatrix}(1+\mu_{min})\mathbf{I}_{3\times3} & \varepsilon\mathbf{I}_{3\times3}\\ \varepsilon\mathbf{I}_{3\times3} & \mathbf{K}_p^{-1}\mathbf{J}\end{bmatrix}\begin{bmatrix}\boldsymbol{\zeta}\\ \boldsymbol{\Omega}_b\end{bmatrix}\right\rangle\\ &= \boldsymbol{\xi}^T\mathbf{P}_{\varepsilon mod}\boldsymbol{\xi}.\end{aligned} \tag{46}$$

The definition of μ_{min} and its role will be clear later in this section. To proceed, let us ignore the disturbance first. Adding $\mathbf{u}$ (the compensation) into equation (17) results in

$$\mathbf{J}\dot{\boldsymbol{\Omega}}_b = -\boldsymbol{\Omega}_b\times\mathbf{J}\boldsymbol{\Omega}_b+\boldsymbol{\tau}+\mathbf{u}. \tag{47}$$

With this, the closed-loop system dynamics becomes

$$\dot{\boldsymbol{\Omega}}_b = -\mathbf{J}^{-1}\mathbf{K}_p\boldsymbol{\zeta}-\mathbf{J}^{-1}\mathbf{K}_d\boldsymbol{\Omega}_b+\mathbf{J}^{-1}\mathbf{u} \tag{48}$$

Therefore, the derivative of (46) is

$$\begin{aligned}\dot{W} &= (1+\mu_{\min})\langle\boldsymbol{\zeta},\boldsymbol{\Omega}_b\rangle+\langle\boldsymbol{\Omega}_b,\mathbf{K}_p^{-1}\mathbf{J}\dot{\boldsymbol{\Omega}}_b\rangle\\ &\quad+\varepsilon\left\langle(\beta_{\hat{\boldsymbol{\zeta}}}\hat{\boldsymbol{\Omega}}_b)^\vee,\boldsymbol{\Omega}_b\right\rangle+\varepsilon\langle\boldsymbol{\zeta},\dot{\boldsymbol{\Omega}}_b\rangle\\ &\le(1+\mu_{\min})\langle\boldsymbol{\zeta},\boldsymbol{\Omega}_b\rangle+\varepsilon\langle\boldsymbol{\Omega}_b,\boldsymbol{\Omega}_b\rangle\\ &\quad+\left\langle\boldsymbol{\Omega}_b,\mathbf{K}_p^{-1}\mathbf{J}\left(-\mathbf{J}^{-1}\mathbf{K}_p\boldsymbol{\zeta}-\mathbf{J}^{-1}\mathbf{K}_d\boldsymbol{\Omega}_b\right)+\mathbf{J}^{-1}\mathbf{u}\right)\right\rangle\\ &\quad+\varepsilon\left\langle\boldsymbol{\zeta},-\mathbf{J}^{-1}\mathbf{K}_p\boldsymbol{\zeta}-\mathbf{J}^{-1}\mathbf{K}_d\boldsymbol{\Omega}_b+\mathbf{J}^{-1}\mathbf{u}\right\rangle\\ &\le-\left\langle\begin{bmatrix}\boldsymbol{\zeta}\\ \boldsymbol{\Omega}_b\end{bmatrix},\mathbf{Q}_\varepsilon\begin{bmatrix}\boldsymbol{\zeta}\\ \boldsymbol{\Omega}_b\end{bmatrix}\right\rangle+\mu_{\min}\langle\boldsymbol{\zeta},\boldsymbol{\Omega}_b\rangle\\ &\quad+\varepsilon\langle\boldsymbol{\zeta},\mathbf{J}^{-1}\mathbf{u}\rangle+\langle\boldsymbol{\Omega}_b,\mathbf{K}_p^{-1}\mathbf{u}\rangle,\end{aligned} \tag{49}$$

where $\mathbf{Q}_\varepsilon$ is as in (36).

For simplicity, let us write

$$\Delta_{\mathbf{u}} = \mu_{min}\langle\boldsymbol{\zeta},\boldsymbol{\Omega}_b\rangle+\varepsilon\left\langle\boldsymbol{\zeta},\mathbf{J}^{-1}\mathbf{u}\right\rangle+\left\langle\boldsymbol{\Omega}_b,\mathbf{K}_p^{-1}\mathbf{u}\right\rangle. \tag{50}$$

Let us work on $\Delta_{\mathbf{u}}$ first. Substituting (44) into (50) yields

$$\begin{aligned}\Delta_{\mathbf{u}} &= \mu_{min}\langle\boldsymbol{\zeta},\boldsymbol{\Omega}_b\rangle\\ &\quad+\varepsilon\left\langle\boldsymbol{\zeta},-\frac{\delta\left(\mathbf{J}^{-1}\mathbf{K}_p\boldsymbol{\zeta}+\mathbf{J}^{-1}\mathbf{K}_p\boldsymbol{\Omega}_b\right)}{\|\mathbf{K}_p\boldsymbol{\zeta}+\mathbf{K}_p\boldsymbol{\Omega}_b\|+\kappa}\right\rangle\\ &\quad+\left\langle\boldsymbol{\Omega}_b,-\frac{\delta\left(\mathbf{K}_p^{-1}\mathbf{K}_p\boldsymbol{\zeta}+\mathbf{K}_p^{-1}\mathbf{K}_p\boldsymbol{\Omega}_b\right)}{\|\mathbf{K}_p\boldsymbol{\zeta}+\mathbf{K}_p\boldsymbol{\Omega}_b\|+\kappa}\right\rangle\\ &= \mu_{min}\langle\boldsymbol{\zeta},\boldsymbol{\Omega}_b\rangle-\frac{\varepsilon\delta}{\|\mathbf{K}_p\boldsymbol{\zeta}+\mathbf{K}_p\boldsymbol{\Omega}_b\|+\kappa}\\ &\quad\times\left(\langle\boldsymbol{\zeta},\mathbf{J}^{-1}\mathbf{K}_p\boldsymbol{\zeta}\rangle+\langle\boldsymbol{\zeta},\mathbf{J}^{-1}\mathbf{K}_p\boldsymbol{\Omega}_b\rangle\right)\\ &\quad-\frac{\delta}{\|\mathbf{K}_p\boldsymbol{\zeta}+\mathbf{K}_p\boldsymbol{\Omega}_b\|+\kappa}\\ &\quad\times\left(\langle\boldsymbol{\zeta},\boldsymbol{\Omega}_b\rangle+\langle\boldsymbol{\Omega}_b,\boldsymbol{\Omega}_b\rangle\right).\end{aligned} \tag{51}$$

Note that the notation "$\times$" in (51) does not mean cross product, but scalar multiplication. Next, let us observe the second line of equation (51). It is apparent that the matrix $\mathbf{K}_p$ multiplied by $\boldsymbol{\zeta}$ and $\boldsymbol{\Omega}_b$ is needed to cancel $\mathbf{K}_p^{-1}$, which is why $\mathbf{K}_p$ is multiplied by $\boldsymbol{\zeta}$ and $\boldsymbol{\Omega}_b$ in equation (44). Next, to ease our calculation, let

$$\mu = \frac{\delta}{\|\mathbf{K}_p\boldsymbol{\zeta}+\mathbf{K}_p\boldsymbol{\Omega}_b\|+\kappa}, \tag{52}$$

so (51) becomes

$$\begin{aligned}\Delta_{\mathbf{u}} &= \mu_{\min}\langle\boldsymbol{\zeta},\boldsymbol{\Omega}_b\rangle \\ &\quad -\mu\varepsilon\left(\langle\boldsymbol{\zeta},\mathbf{J}^{-1}\mathbf{K}_p\boldsymbol{\zeta}\rangle+\langle\boldsymbol{\zeta},\mathbf{J}^{-1}\mathbf{K}_p\boldsymbol{\Omega}_b\rangle\right) \\ &\quad -\mu\langle\boldsymbol{\zeta},\boldsymbol{\Omega}_b\rangle-\mu\langle\boldsymbol{\Omega}_b,\boldsymbol{\Omega}_b\rangle. \end{aligned} \tag{53}$$

From (52), the values of δ, $\boldsymbol{\zeta}$, and $\boldsymbol{\Omega}_b$ are limited or finite. Thus, it is safe to assume that the angle $\boldsymbol{\zeta}$ has limited range, e.g. from -2π (clockwise full circle rotation) to 2π (counterclockwise full circle rotation). Meanwhile, $\boldsymbol{\Omega}_b$ is obviously limited because quadrotor has maximum angular velocity. This maximum angular velocity is due to motor, propeller, and aerodynamics limitation. Therefore, the bounds of μ can be written as

$$\mu_{\min}\le\mu\le\mu_{\max}, \tag{54}$$

which implies that

$$-\mu_{\max}\le-\mu\le-\mu_{\min}. \tag{55}$$

The maximum value $\mu_{\max}$ occurs when the denominator of μ, i.e., $(\|\mathbf{K}_p\boldsymbol{\zeta}+\mathbf{K}_p\boldsymbol{\Omega}_b\|+\kappa)$, reaches its minimum, which happens when both $\boldsymbol{\zeta}$ and $\boldsymbol{\Omega}_b$ reach $\mathbf{0}$. On the other hand, the minimum value $\mu_{\min}$ occurs when the denominator of μ reaches its maximum value, which happens when $\boldsymbol{\zeta}$ and $\boldsymbol{\Omega}_b$ reach their maximum values (i.e., $\boldsymbol{\zeta}_{\max}$ and $\boldsymbol{\Omega}_{b\max}$). Mathematically, $\mu_{\min}$ can be written as

$$\mu_{\min}=\frac{\delta}{\|\mathbf{K}_p\boldsymbol{\zeta}_{\max}+\mathbf{K}_p\boldsymbol{\Omega}_{b\max}\|+\kappa}. \tag{56}$$

Next, we have to modify equation (53) so that we can write it in quadratic form. For simplicity, let us write

$$\begin{aligned}\eta &= \left(\langle\boldsymbol{\zeta},\mathbf{J}^{-1}\mathbf{K}_p\boldsymbol{\zeta}\rangle+\langle\boldsymbol{\zeta},\mathbf{J}^{-1}\mathbf{K}_p\boldsymbol{\Omega}_b\rangle\right), \\ \upsilon &= \langle\boldsymbol{\Omega}_b,\boldsymbol{\Omega}_b\rangle. \end{aligned} \tag{57}$$

Equation (53) has an upper bound of

$$\begin{aligned}\Delta_{\mathbf{u}} &\le -\mu\varepsilon\eta-\mu_{\min}\langle\boldsymbol{\zeta},\boldsymbol{\Omega}_b\rangle-\mu\upsilon \\ &\quad +\mu_{min}\langle\boldsymbol{\zeta},\boldsymbol{\Omega}_b\rangle \\ &\le -\mu\varepsilon\eta-\mu\upsilon. \end{aligned} \tag{58}$$

In (58), the term $\mu_{\min}\langle\boldsymbol{\zeta},\boldsymbol{\Omega}_b\rangle$ cancels the term $-\mu_{\min}\langle\boldsymbol{\zeta},\boldsymbol{\Omega}_b\rangle$. The term $+\mu_{\min}\langle\boldsymbol{\zeta},\boldsymbol{\Omega}_b\rangle$ comes from the term $\mu_{\min}$ in the upper left corner of $\mathbf{P}_{\varepsilon mod}$ (equation (46)), which shows the reason for the introduction of $\mu_{\min}$ in $\mathbf{P}_{\varepsilon mod}$.

Let us expand $\Delta_{\mathbf{u}}$ again as

$$\begin{aligned}\Delta_{\mathbf{u}} &\le -\mu\varepsilon\left(\langle\boldsymbol{\zeta},\mathbf{J}^{-1}\mathbf{K}_p\boldsymbol{\zeta}\rangle+\mathbf{K}_p\langle\boldsymbol{\zeta},\mathbf{J}^{-1}\boldsymbol{\Omega}_b\rangle\right) \\ &\quad -\mu\mathbf{K}_p\langle\boldsymbol{\Omega}_b,\mathbf{K}_p^{-1}\boldsymbol{\Omega}_b\rangle \\ &\le -\mu\begin{bmatrix}\boldsymbol{\zeta}\\ \boldsymbol{\Omega}_b\end{bmatrix}^T\begin{bmatrix}\mathbf{J}^{-1}\mathbf{K}_p & 0.5\varepsilon\mathbf{K}_p\mathbf{J}^{-1}\\ 0.5\varepsilon\mathbf{K}_p\mathbf{J}^{-1} & \mathbf{I}_{3\times3}\end{bmatrix}\begin{bmatrix}\boldsymbol{\zeta}\\ \boldsymbol{\Omega}_b\end{bmatrix} \\ &\le -\mu\boldsymbol{\xi}^T\mathbf{S}_\varepsilon\boldsymbol{\xi} \\ &\le -\mu_{\min}\boldsymbol{\xi}^T\mathbf{S}_\varepsilon\boldsymbol{\xi}, \end{aligned} \tag{59}$$

where

$$\mathbf{S}_\varepsilon = \begin{bmatrix}\mathbf{J}^{-1}\mathbf{K}_p & 0.5\varepsilon\mathbf{K}_p\mathbf{J}^{-1}\\ 0.5\varepsilon\mathbf{K}_p\mathbf{J}^{-1} & \mathbf{I}_{3\times3}\end{bmatrix}. \tag{60}$$

For sufficiently small ε, $\mathbf{S}_\varepsilon$ is a positive definite matrix. Next, using (59), equation (49) can be written as

$$\begin{aligned}\dot{W} &\le -\boldsymbol{\xi}^T\mathbf{Q}_\varepsilon\boldsymbol{\xi}-\mu\boldsymbol{\xi}^T\mathbf{S}_\varepsilon\boldsymbol{\xi} \\ &\le -\boldsymbol{\xi}^T\mathbf{Q}_\varepsilon\boldsymbol{\xi}-\mu_{\min}\boldsymbol{\xi}^T\mathbf{S}_\varepsilon\boldsymbol{\xi}, \end{aligned} \tag{61}$$

which shows the negative definiteness of $\dot{W}$.

Let us proceed to Lyapunov analysis if the disturbance is present. If there is a disturbance $\mathbf{g}$, (47) is changed into

$$\mathbf{J}\dot{\boldsymbol{\Omega}}_b=-\boldsymbol{\Omega}_b\times\mathbf{J}\boldsymbol{\Omega}_b+\boldsymbol{\tau}+\mathbf{u}+\mathbf{g}. \tag{62}$$

Then the closed-loop system dynamics becomes

$$\dot{\boldsymbol{\Omega}}_b = -\mathbf{J}^{-1}\mathbf{K}_p\boldsymbol{\zeta}-\mathbf{J}^{-1}\mathbf{K}_d+\mathbf{J}^{-1}\mathbf{u}+\mathbf{J}^{-1}\mathbf{g}. \tag{63}$$

The introduction of $\mathbf{u}$ adds the term $\varepsilon\langle\boldsymbol{\zeta},\mathbf{J}^{-1}\mathbf{u}\rangle+\langle\boldsymbol{\Omega}_b,\mathbf{K}_p^{-1}\mathbf{u}\rangle$ in (49). Similarly, the introduction of $\mathbf{g}$ adds the term $\Delta_{\mathbf{g}}$, i.e.

$$\Delta_{\mathbf{g}}=\varepsilon\langle\boldsymbol{\zeta},\mathbf{J}^{-1}\mathbf{g}\rangle+\langle\boldsymbol{\Omega}_b,\mathbf{K}_p^{-1}\mathbf{g}\rangle. \tag{64}$$

This term modifies (61) to

$$\dot{W} \le -\boldsymbol{\xi}^T\mathbf{Q}_\varepsilon\boldsymbol{\xi}-\mu\boldsymbol{\xi}^T\mathbf{S}_\varepsilon\boldsymbol{\xi}+\Delta_{\mathbf{g}}. \tag{65}$$

Equation (65) shows that the negative definiteness of the quadrotor system is not guaranteed if the unknown disturbance $\mathbf{g}$ is present. Physically, it means that quadrotor (or any flying object) cannot be expected to be perfectly still under the influence of unknown disturbance. However, we can expect the state variables to be bounded, and the bound shall reduce if the compensation is introduced. To conduct the bound analysis, we use this following lemma from [23], which is about the bound of state variables if disturbance is present (its proof can be seen at [23] as well).

Lemma 1: Let the nominal system

$$\dot{\mathbf{x}}=\mathbf{f}(t,\mathbf{x}) \tag{66}$$

has an exponentially stable equilibrium point at $\mathbf{x}=\mathbf{0}$. Also let $W(t,\mathbf{x})$ be the system's nominal Lyapunov function that satisfies

$$c_1\|\mathbf{x}\|^2\le W(t,\mathbf{x})\le c_2\|\mathbf{x}\|^2, \tag{67}$$

$$\frac{\partial W}{\partial t}+\frac{\partial W}{\partial\mathbf{x}}\mathbf{f}(t,\mathbf{x})\le-c_3\|\mathbf{x}\|^2, \tag{68}$$

$$\frac{\partial W}{\partial\mathbf{x}}\le c_4\|\mathbf{x}\|^2, \tag{69}$$

in $[0,\infty]\times D$, $D=\{\mathbf{x}\in\Re^n|\,\|\mathbf{x}\|<r\}$. For all $t\ge0$, all $\mathbf{x}\in D$, and $0<\Theta<1$, the system is perturbed by $\mathbf{g}(t,\mathbf{x})$ as

$$\dot{\mathbf{x}}=\mathbf{f}(t,\mathbf{x})+\mathbf{g}(t,\mathbf{x}), \tag{70}$$

where the perturbation $\mathbf{g}(t,\mathbf{x})$ satisfies

$$\|\mathbf{g}(t,\mathbf{x})\| \leq \Phi < \frac{c_3}{c_4}\sqrt{\frac{c_1}{c_2}}\Theta r. \tag{71}$$

Then, for all $\|\mathbf{x}(t_0)\| < (\sqrt{c_1/c_2})r$ and for some finite T, the solution of (70) satisfies

$$\|\mathbf{x}(t)\| \leq k\exp[-\gamma(t-t_0)]\,\|\mathbf{x}(t_0)\|, \tag{72}$$

for all $t_0 \leq t < t_0+T$, and

$$\|\mathbf{x}(t)\| \leq b, \tag{73}$$

for all $t \geq t_0+T$. The constants k, γ, and b are

$$\begin{aligned} k &= \sqrt{\frac{c_1}{c_2}}, \\ \gamma &= \frac{(1-\Theta)c_3}{2c_2}, \\ b &= \frac{c_4}{c_3}\sqrt{\frac{c_2}{c_1}}\frac{\Phi}{\Theta}. \end{aligned}$$

With Lemma 1 in mind, we can conduct the bound analysis. First, we conduct the analysis with nominal PD control law in (21) using the Lyapunov function in (28) and the Lyapunov time derivative in (35). After that, we use the PD control law (21) with compensation $\mathbf{u}$; for this, we will use the modified Lyapunov function in (46) and its derivative in (61). In both cases, we shall calculate c_1 to c_4 in Lemma 1. To distinguish one case from the other, the first case is denoted with roman number subscript "I", while the second case with roman number subscript "II". Therefore, for the first case, we calculate c_{1I} to c_{4I}, while for the second case, c_{1II} to c_{4II}.

Let us proceed to the first case. The values of c_{1I} to c_{4I} are

$$\begin{aligned} c_{1I} &= \lambda_{\min}(\mathbf{P}_\varepsilon), \\ c_{2I} &= \lambda_{\max}(\mathbf{P}_\varepsilon), \\ c_{3I} &= \lambda_{\min}(\mathbf{Q}_\varepsilon), \\ c_{4I} &= 2\lambda_{\max}(\mathbf{P}_\varepsilon). \end{aligned} \tag{74}$$

From (72), the bound can be calculated as

$$\|\mathbf{x}(t)\|_I \leq k_I\exp[-\gamma_I(t-t_0)]\,\|\mathbf{x}(t_0)\|, \tag{75}$$

for $t_0 \leq t < t_0+T$ and

$$\|\mathbf{x}(t)\|_I \leq b_I, \tag{76}$$

for all $t \geq t_0+T$. Here, k, γ, and b are

$$\begin{aligned} k_I &= \sqrt{\frac{c_{1I}}{c_{2I}}}, \\ \gamma_I &= \frac{(1-\Theta)c_{3I}}{2c_{2I}}, \\ b_I &= \frac{c_{4I}}{c_{3I}}\sqrt{\frac{c_{2I}}{c_{1I}}}\frac{\Phi}{\Theta}. \end{aligned} \tag{77}$$

Next, let us proceed to the second case. The values of c_{1II} to c_{4II} are

$$\begin{aligned} c_{1II} &= \lambda_{\min}(\mathbf{P}_{\varepsilon mod}), \\ c_{2II} &= \lambda_{\max}(\mathbf{P}_{\varepsilon mod}), \\ c_{3II} &= \lambda_{\min}(\mathbf{Q}_\varepsilon) + \mu_{\min}\lambda_{\max}(\mathbf{S}_\varepsilon), \\ c_{4II} &= 2\lambda_{\max}(\mathbf{P}_{\varepsilon mod}). \end{aligned} \tag{78}$$

Also from (72), the bound in our problem can also be found as

$$\|\mathbf{x}(t)\|_{II} \leq k_{II}\exp[-\gamma_{II}(t-t_0)]\,\|\mathbf{x}(t_0)\|, \tag{79}$$

for $t_0 \leq t < t_0+T$ and

$$\|\mathbf{x}(t)\|_{II} \leq b_{II}, \tag{80}$$

for all $t \geq t_0+T$. Here, k, γ, and b are

$$\begin{aligned} k_{II} &= \sqrt{\frac{c_{1II}}{c_{2II}}}, \\ \gamma_{II} &= \frac{(1-\Theta)c_{3II}}{2c_{2II}}, \\ b_{II} &= \frac{c_{4II}}{c_{3II}}\sqrt{\frac{c_{2II}}{c_{1II}}}\frac{\Delta}{\Theta}. \end{aligned} \tag{81}$$

In principle it is hard to find the exact values of c_{1I} to c_{4I} and c_{1II} to c_{4II} even using symbolic tools. Therefore, in this paper, they will be verified using numerical study in Section 5.

4.3. PD control under inertia matrix perturbation

As in real situations, quadrotor inertia matrix may not be known exactly. In this section, we redefine $\mathbf{J}$ differently from that in Section 4.1 and 4.2. Previously, in those sections, we assumed that the knowledge of the inertia matrix is perfect (there is no inertia matrix perturbation). Here, it is assumed we only have the knowledge of $\mathbf{J}_0$ (called the nominal inertia matrix) and the true value of inertia matrix $\mathbf{J}$ is left unknown. The inertia matrix perturbation is called $\Delta\mathbf{J}$, defined as

$$\mathbf{J} = \mathbf{J}_0 + \Delta\mathbf{J}, \tag{82}$$

where $\Delta\mathbf{J}$ does not have to be diagonal, but symmetric.

The control law $\boldsymbol{\tau}$ is designed using the nominal inertia matrix $\mathbf{J}_0$ as

$$\boldsymbol{\tau} = \boldsymbol{\Omega}_b \times \mathbf{J}_0\boldsymbol{\Omega}_b - \mathbf{K}_p\boldsymbol{\zeta} - \mathbf{K}_d\boldsymbol{\Omega}_b. \tag{83}$$

With the presence of the perturbation, the dynamics of the system becomes

$$\begin{aligned} \mathbf{J}\dot{\boldsymbol{\Omega}}_b &= -\boldsymbol{\Omega}_b \times \mathbf{J}\boldsymbol{\Omega}_b + \boldsymbol{\tau} \\ \mathbf{J}\dot{\boldsymbol{\Omega}}_b &= -\boldsymbol{\Omega}_b \times (\mathbf{J}_0 + \Delta\mathbf{J})\boldsymbol{\Omega}_b + \\ &\qquad \boldsymbol{\Omega}_b \times \mathbf{J}_0\boldsymbol{\Omega}_b - \mathbf{K}_p\boldsymbol{\zeta} - \mathbf{K}_d\boldsymbol{\Omega}_b \\ \mathbf{J}\dot{\boldsymbol{\Omega}}_b &= -\boldsymbol{\Omega}_b \times \Delta\mathbf{J}\boldsymbol{\Omega}_b \end{aligned}$$

$$
\begin{aligned}
&-\mathbf{K}_p\boldsymbol{\zeta}-\mathbf{K}_d\boldsymbol{\Omega}_b\\
\dot{\boldsymbol{\Omega}}_b=&-\mathbf{J}^{-1}(\boldsymbol{\Omega}_b\times\Delta\mathbf{J}\boldsymbol{\Omega}_b)\\
&-\mathbf{J}^{-1}\mathbf{K}_p\boldsymbol{\zeta}-\mathbf{J}^{-1}\mathbf{K}_d\boldsymbol{\Omega}_b.
\end{aligned}\tag{84}
$$

Here we write $\boldsymbol{\Omega}_b\times\Delta\mathbf{J}\boldsymbol{\Omega}_b$ as a vector, i.e.,

$$
\boldsymbol{\Omega}_b\times\Delta\mathbf{J}\boldsymbol{\Omega}_b=\mathbf{g}'.\tag{85}
$$

Therefore, (84) becomes

$$
\begin{aligned}
\mathbf{J}\dot{\boldsymbol{\Omega}}_b&=-\mathbf{g}'-\mathbf{K}_p\boldsymbol{\zeta}-\mathbf{K}_d\boldsymbol{\Omega}_b\\
\dot{\boldsymbol{\Omega}}_b&=-\mathbf{J}^{-1}\mathbf{g}'-\mathbf{J}^{-1}\mathbf{K}_p\boldsymbol{\zeta}-\mathbf{J}^{-1}\mathbf{K}_d\boldsymbol{\Omega}_b.
\end{aligned}\tag{86}
$$

Equation (85) shows that the perturbation $\Delta\mathbf{J}$ can be represented by a vector $\mathbf{g}'$. By referring to (63), it can be seen that the position of $\mathbf{g}'$ in the dynamics equation is the same as the position of $\mathbf{g}$. This implies that the effect of inertia matrix perturbation is the same as the effect of disturbance. Meanwhile, Section 4.2 demonstrates that any vector disturbance can be countered by the disturbance compensation $\mathbf{u}$ in (44); thus, $\mathbf{u}$ can also handle the inertia matrix perturbation. Therefore, for stabilization case, there is no need of adaptive law to handle inertia matrix perturbation. This is different from [9] and [10] where an adaptive law was proposed to estimate the inertia matrix $\mathbf{J}$.

It is important to note that there is a limit to the perturbation $\Delta\mathbf{J}$. In Section 4.2, it is assumed that $\|\mathbf{g}\|\leq\delta$. Therefore, the magnitude of $\mathbf{g}'$ must be upper-bounded by δ, which means that there is an upper bound for $\|\Delta\mathbf{J}\|$. We can start describing this by writing $\|\boldsymbol{\Omega}_b\times\Delta\mathbf{J}\boldsymbol{\Omega}_b\|$ in more detail, i.e.,

$$
\begin{aligned}
\|\boldsymbol{\Omega}_b\times\Delta\mathbf{J}\boldsymbol{\Omega}_b\|&\leq\|\boldsymbol{\Omega}_b\|\,\|\Delta\mathbf{J}\boldsymbol{\Omega}_b|\\
&\leq\|\boldsymbol{\Omega}_b\|\,\|\Delta\mathbf{J}\|\,\|\boldsymbol{\Omega}_b|\\
&\leq\|\boldsymbol{\Omega}_b\|^2\,\|\Delta\mathbf{J}\|,
\end{aligned}\tag{87}
$$

where we use the induced norm for $\Delta\mathbf{J}$. Next, we can assume that the magnitude of body angular velocity is limited by $\|\boldsymbol{\Omega}_b\|_{\max}$ because of motor, propeller, and aerodynamic limitation. Therefore, (87) can be rewritten as

$$
\|\boldsymbol{\Omega}_b\times\Delta\mathbf{J}\boldsymbol{\Omega}_b\|\leq\|\boldsymbol{\Omega}_b\|_{\max}^2\,\|\Delta\mathbf{J}\|.\tag{88}
$$

Because $\|\mathbf{g}'\|\leq\delta$, we can write

$$
\begin{aligned}
\|\boldsymbol{\Omega}_b\|_{\max}^2\,\|\Delta\mathbf{J}\|&\leq\delta\\
\|\Delta\mathbf{J}\|&\leq\frac{\delta}{\|\boldsymbol{\Omega}_b\|_{\max}^2}.
\end{aligned}\tag{89}
$$

An interesting phenomenon happens when $\mathbf{K}_p$ is diagonal and all of its elements are equal, and $\Delta\mathbf{J}$ is also diagonal, i.e.,

$$
\Delta\mathbf{J}=\begin{bmatrix}\Delta J_{xx}&0&0\\0&\Delta J_{yy}&0\\0&0&\Delta J_{zz}\end{bmatrix}.\tag{90}
$$

Here we still maintain the nominal PD control law in (21) without compensation as our controller. Substituting (84) into the time derivative of (28) yields

$$
\begin{aligned}
\dot{W}=&\langle\boldsymbol{\zeta},\boldsymbol{\Omega}_b\rangle+\left\langle\boldsymbol{\Omega}_b,\mathbf{K}_p^{-1}\mathbf{J}\dot{\boldsymbol{\Omega}}_b\right\rangle\\
&+\varepsilon\left\langle(\beta_{\hat{\boldsymbol{\zeta}}}\hat{\boldsymbol{\Omega}}_b)^{\vee},\boldsymbol{\Omega}_b\right\rangle+\varepsilon\left\langle\boldsymbol{\zeta},\dot{\boldsymbol{\Omega}}_b\right\rangle\\
\leq&-\left\langle\boldsymbol{\Omega}_b,\mathbf{K}_p^{-1}\mathbf{K}_d\boldsymbol{\Omega}_b\right\rangle+\varepsilon\left\langle\boldsymbol{\Omega}_b,\boldsymbol{\Omega}_b\right\rangle\\
&-\varepsilon\left\langle\boldsymbol{\zeta},\mathbf{J}^{-1}\mathbf{K}_p\boldsymbol{\zeta}\right\rangle-\varepsilon\left\langle\boldsymbol{\zeta},\mathbf{J}^{-1}\mathbf{K}_d\boldsymbol{\Omega}_b\right\rangle\\
&-\left\langle\boldsymbol{\Omega}_b,\mathbf{K}_p^{-1}\boldsymbol{\Omega}_b\times\Delta\mathbf{J}\boldsymbol{\Omega}_b\right\rangle-\varepsilon\left\langle\boldsymbol{\zeta},\mathbf{J}^{-1}\boldsymbol{\Omega}_b\times\Delta\mathbf{J}\boldsymbol{\Omega}_b\right\rangle\\
\leq&-\boldsymbol{\xi}^T\mathbf{Q}_\varepsilon\boldsymbol{\xi}-\varepsilon\left\langle\boldsymbol{\zeta},\mathbf{J}^{-1}\boldsymbol{\Omega}_b\times\Delta\mathbf{J}\boldsymbol{\Omega}_b\right\rangle\\
&-\left\langle\boldsymbol{\Omega}_b,\mathbf{K}_p^{-1}\boldsymbol{\Omega}_b\times\Delta\mathbf{J}\boldsymbol{\Omega}_b\right\rangle\\
\leq&-\boldsymbol{\xi}^T\mathbf{Q}_\varepsilon\boldsymbol{\xi}+\Xi_1+\Xi_2,
\end{aligned}\tag{91}
$$

where the last term is

$$
\begin{aligned}
\Xi_2=&-(\Delta J_1/k_{p3}-\Delta J_1/k_{p2}\\
&+\Delta J_2/k_{p1}-\Delta J_2/k_{p3}\\
&+\Delta J_3/k_{p2}-\Delta J_3/k_{p1})pqr.
\end{aligned}\tag{92}
$$

The derivation of Ξ_1 and Ξ_2 can be conducted by using symbolic computation software such as MATLAB symbolic computation tool. The term Ξ_2 can be made zero if $k_{p1}=k_{p2}=k_{p3}$. The term Ξ_1 is sign-indefinite. However, because ε is small, it can be assumed that Ξ_1 does not disturb system stability significantly.

The preceding analysis can be extended to know how large the perturbation that can cause system instability. In this analysis, it is assumed that $k_{p1}=k_{p2}=k_{p3}$ so that $\Xi_2=0$. Therefore, the only term that can cause instability is Ξ_1. Rewriting (92) yields

$$
\begin{aligned}
\dot{W}&\leq-\boldsymbol{\xi}^T\mathbf{Q}_\varepsilon\boldsymbol{\xi}+\Xi_1\\
&\leq-\boldsymbol{\xi}^T\mathbf{Q}_\varepsilon\boldsymbol{\xi}-\varepsilon\left\langle\boldsymbol{\xi},\mathbf{J}^{-1}\boldsymbol{\Omega}_b\times\Delta\mathbf{J}\boldsymbol{\Omega}_b\right\rangle.
\end{aligned}\tag{93}
$$

The second term in the right-hand side of (93) has an upper bound of

$$
\begin{aligned}
\Xi_1&=-\varepsilon\left\langle\boldsymbol{\xi},\mathbf{J}^{-1}\boldsymbol{\Omega}_b\times\Delta\mathbf{J}\boldsymbol{\Omega}_b\right\rangle\\
&\leq\varepsilon\,\|\boldsymbol{\zeta}\|\left\|\mathbf{J}^{-1}\boldsymbol{\Omega}_b\right\|\|\Delta\mathbf{J}\boldsymbol{\Omega}_b\|\\
&\leq\varepsilon\,\|\boldsymbol{\zeta}\|\left\|\mathbf{J}^{-1}\right\|\|\Delta\mathbf{J}\|\,\|\boldsymbol{\Omega}_b\|^2,
\end{aligned}\tag{94}
$$

and the first term of (93) has an upper bound of

$$
-\boldsymbol{\xi}^T\mathbf{Q}_\varepsilon\boldsymbol{\xi}\leq-\lambda_{\min}\|\boldsymbol{\xi}\|^2.\tag{95}
$$

With (94) and (95) in mind, and by noting that

$$
\|\boldsymbol{\xi}\|^2=\|\boldsymbol{\zeta}\|^2+\|\boldsymbol{\Omega}_b\|^2,\tag{96}
$$

inequality (93) becomes

$$
\begin{aligned}
\dot{W}&\leq-\lambda_{\min}(\mathbf{Q}_\varepsilon)\|\boldsymbol{\xi}\|^2+\varepsilon\,\|\boldsymbol{\zeta}\|\left\|\mathbf{J}^{-1}\right\|\|\Delta\mathbf{J}\|\,\|\boldsymbol{\Omega}_b\|^2\\
&\leq-\lambda_{\min}(\mathbf{Q}_\varepsilon)\|\boldsymbol{\zeta}\|^2-\lambda_{\min}(\mathbf{Q}_\varepsilon)\|\boldsymbol{\Omega}_b\|^2\\
&\quad+\varepsilon\,\|\boldsymbol{\zeta}\|\left\|\mathbf{J}^{-1}\right\|\|\Delta\mathbf{J}\|\,\|\boldsymbol{\Omega}_b\|^2.
\end{aligned}\tag{97}
$$

The stability of the system will be disturbed if the right-hand side of (97) becomes positive. Therefore, to ensure that $\dot{W}$ is negative definite, $\|\Delta\mathbf{J}\|$ has to fulfill

$$
0>-\lambda_{\min}(\mathbf{Q}_\varepsilon)(\|\boldsymbol{\zeta}\|^2+\|\boldsymbol{\Omega}_b\|^2)
$$

$$
\begin{aligned}
&+\varepsilon\|\boldsymbol{\zeta}\|\left\|\mathbf{J}^{-1}\right\|\|\Delta\mathbf{J}\|\|\boldsymbol{\Omega}_b\|^2,\\
\|\Delta\mathbf{J}\| &< \frac{\lambda_{\min}(\mathbf{Q}_\varepsilon)\left(\|\boldsymbol{\zeta}\|^2+\|\Omega_b\|^2\right)}{\varepsilon\|\mathbf{J}^{-1}\|\|\boldsymbol{\zeta}\|\|\boldsymbol{\Omega}_b\|^2}\\
&< h(\|\boldsymbol{\zeta}\|,\|\boldsymbol{\Omega}_b\|). \qquad (98)
\end{aligned}
$$

Equation (98) says that $\|\Delta\mathbf{J}\|$ must be less than $h(\|\boldsymbol{\zeta}\|,\|\boldsymbol{\Omega}_b\|)$ to guarantee the system's asymptotic stability.

4.4. Control algorithm under disturbance and inertia matrix perturbation

Sections 4.2 and 4.3 show that the compensation $\mathbf{u}$ can handle both disturbance and inertia matrix perturbation. However, each of the sections only considers external disturbance and inertia matrix separately. In Section 4.2, the external disturbance is represented by the vector variable $\mathbf{g}$. Meanwhile, in Section 4.3, the inertia matrix perturbation yields a vector $\mathbf{g}'$. Both sections assumed that each of $\|\mathbf{g}\|$ and $\|\mathbf{g}'\|$ has an upper bound of δ.

Let us define another vector variable

$$\mathbf{g}_{tot}=\mathbf{g}+\mathbf{g}'. \qquad (99)$$

We also need to redefine the upper bound of $\|\mathbf{g}\|$ and $\|\mathbf{g}'\|$ as

$$
\begin{aligned}
\|\mathbf{g}\| &\le \delta_1,\\
\|\mathbf{g}'\| &\le \delta_2. \qquad (100)
\end{aligned}
$$

Using triangle inequality, the upper bound of $\|\mathbf{g}_{tot}\|$ is

$$\|\mathbf{g}_{tot}\|\le\|\mathbf{g}\|+\|\mathbf{g}'\|\le\delta_1+\delta_2=\delta_{tot}. \qquad (101)$$

If the total disturbance is caused by external disturbance and inertia matrix perturbation, the variable δ in compensation $\mathbf{u}$ in (44) has to be changed to δ_{tot}:

$$\mathbf{u}=-\frac{\delta_{tot}\left(\mathbf{K}_p\boldsymbol{\zeta}+\mathbf{K}_p\boldsymbol{\Omega}_b\right)}{\|\mathbf{K}_p\boldsymbol{\zeta}+\mathbf{K}_p\boldsymbol{\Omega}_b\|+\kappa}. \qquad (102)$$

Therefore, the design and analysis of the controller is completed. To conclude this section, we write the final form of the controller with compensation, i.e., $\tau+\mathbf{u}$, as

$$
\begin{aligned}
\tau+\mathbf{u} &= \boldsymbol{\Omega}_b\times\mathbf{J}\boldsymbol{\Omega}_b-\mathbf{K}_p\boldsymbol{\zeta}-\mathbf{K}_d\boldsymbol{\Omega}_b\\
&\quad-\frac{\delta_{tot}\left(\mathbf{K}_p\boldsymbol{\zeta}+\mathbf{K}_p\boldsymbol{\Omega}_b\right)}{\|\mathbf{K}_p\boldsymbol{\zeta}+\mathbf{K}_p\boldsymbol{\Omega}_b\|+\kappa}. \qquad (103)
\end{aligned}
$$

5. NUMERICAL SIMULATION AND ANALYSIS

5.1. Numerical values and simulation results

Numerical simulation is conducted by adding disturbance and perturbation to the system. The constants used in equation (10) to (20) are as follows:

$$J_{xx}=0.082\ \text{kg.m}^2,$$

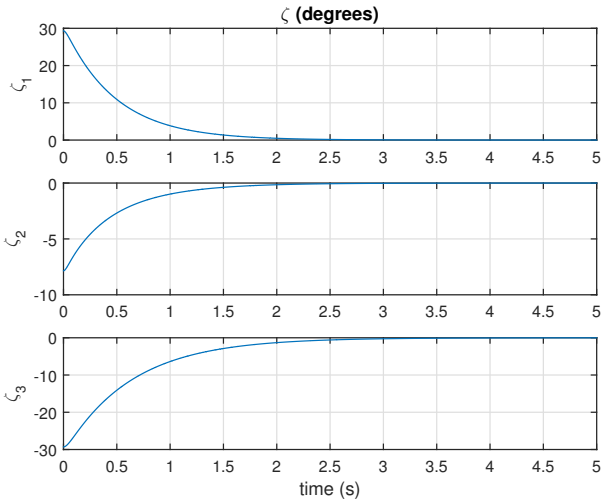

Fig. 3. Angle $\boldsymbol{\zeta}$ with PD control law from (21).

$$J_{yy}=0.0845\ \text{kg.m}^2,$$
$$J_{zz}=0.1377\ \text{kg.m}^2.$$

The simulation is conducted for 5 seconds. The initial conditions are set to $\boldsymbol{\zeta}(0)=\begin{bmatrix}29.31 & -7.85 & -29.31\end{bmatrix}^T$ degrees and $\boldsymbol{\Omega}_b(0)=\mathbf{0}$ degrees/s. The angle unit is given in degrees for convenience. Next, the unit degrees may be abbreviated as deg. Except for simulation no.5 (Fig. 7), the matrix $\mathbf{K}_p$ and $\mathbf{K}_d$ are

$$\mathbf{K}_p = \begin{bmatrix}8&0&0\\0&7&0\\0&0&6\end{bmatrix}, \qquad (104)$$

$$\mathbf{K}_d = 4\mathbf{I}_{3\times3}, \qquad (105)$$

The conducted simulations are given in the following list.

1) Fig. 3 shows the performance of the closed-loop system with the PD controller in equation (21) with no disturbance. The system is asymptotically stable. In the remainder of this paper, this condition is called "nominal condition".
2) The effect of $\kappa=0$ under the absence of disturbance and inertia matrix perturbation is shown in Fig. 4. Although $\boldsymbol{\zeta}$ is stable and convergent, the angular acceleration suffers from chattering. Note that the angular acceleration is $\dot{\boldsymbol{\Omega}}=\frac{d}{dt}\begin{bmatrix}p & q & r\end{bmatrix}^T=\begin{bmatrix}dp/dt & dq/dt & dr/dt\end{bmatrix}^T$. The chattering is apparent as dense red, blue, and green region in Fig. 4. This is why κ should not be set to 0. Therefore, in the next simulations, κ is set to be 0.1. Fig. 5 shows that the chattering vanishes if $\kappa=0.1$. In Fig. 4 and 5, δ_{tot} is equal to 2.17.
3) Fig. 6 shows the angle $\boldsymbol{\zeta}$ under random disturbance, without and with compensation. The value of δ_1 and δ_2 are respectively set to be 2.17 and 0, so $\delta_{tot}=2.17$.

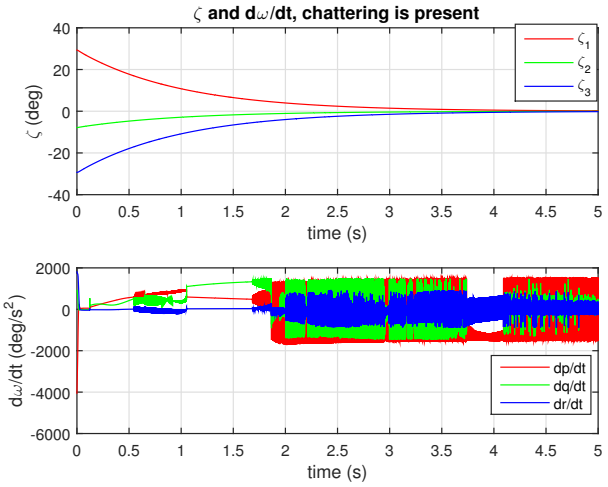

Fig. 4. Angle $\boldsymbol{\zeta}$ and angular acceleration $d\boldsymbol{\omega}/dt$ under PD control law and compensation for $\kappa = 0$, without disturbance. The chattering is present in $d\boldsymbol{\omega}/dt$.

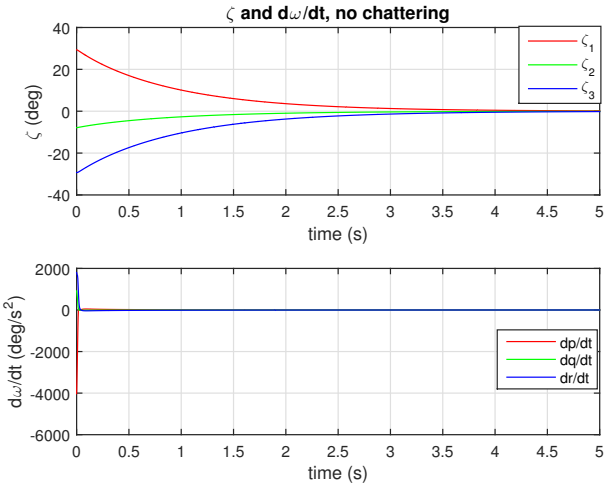

Fig. 5. Angle $\boldsymbol{\zeta}$ and the angular acceleration without chattering, when $\kappa = 0.1$.

This figure demonstrates that the compensation reduces the bound of state variables and improves the system stability. In addition, the vibration (shown by the "wave" in the graph) is also reduced.

4) Fig. 7 shows the simulation under the inertia matrix perturbation (but without disturbance). Here the nominal inertia matrix $\mathbf{J}_0$ is diagonal as in (11), with its elements' values given in the beginning of this section. The perturbation given fulfills the criterion in (89), i.e. $\|\Delta\mathbf{J}\| \leq \delta_2 / \|\boldsymbol{\Omega}_b\|^2_{\max}$ (the variable δ_2 in (89) is used instead of δ because the upper bound for $\|\mathbf{g}'\|$ is δ_2, as in (100)). The value of δ_2 is set to 2, while $\boldsymbol{\Omega}_{b\max}$ is set to be $\begin{bmatrix} \pi/3 & \pi/3 & \pi/3 \end{bmatrix}^T$, which makes $\|\boldsymbol{\Omega}_{b\max}\| = \pi\sqrt{3}/3$. Therefore $\|\Delta\mathbf{J}\| \leq 0.61$. Here we give $\Delta\mathbf{J}$:

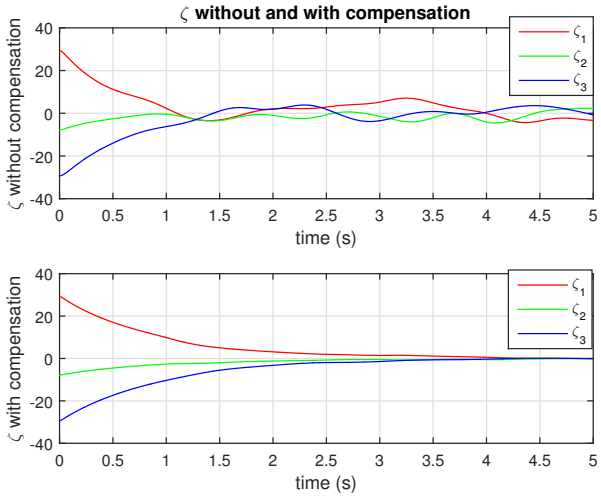

Fig. 6. Angle $\boldsymbol{\zeta}$ without compensation (above) and with compensation (below).

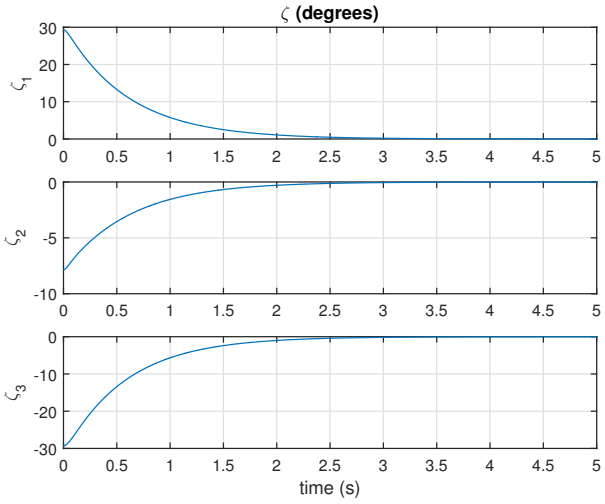

Fig. 7. Angle $\boldsymbol{\zeta}$ if $\Delta\mathbf{J}$ is diagonal and $\mathbf{K}_p$ is diagonal with all of its elements equal.

$$\Delta\mathbf{J} = \begin{bmatrix} 0.09 & 0.18 & 0.135 \\ 0.18 & 0.117 & 0.126 \\ 0.135 & 0.126 & 0.099 \end{bmatrix}. \quad (106)$$

The simulation shows that the disturbance compensation can yield the convergence and stability of the state variables.

5) Fig. 8 shows the simulation if the perturbation $\Delta\mathbf{J}$ is diagonal as in (90), $\mathbf{K}_p$ is diagonal with all of its elements are equal, and disturbance does not occur. The perturbation is $\Delta\mathbf{J} = 0.5\mathbf{J}_0$. For this case, the proportional gain matrix $\mathbf{K}_p$ is set to be equal to $8\mathbf{I}_{3\times3}$, while the derivative constant matrix is $\mathbf{K}_d = 5\mathbf{I}_{3\times3}$. The compensation is not added to the control law. The figure shows that the angle $\boldsymbol{\zeta}$ is stable and convergent to zero.

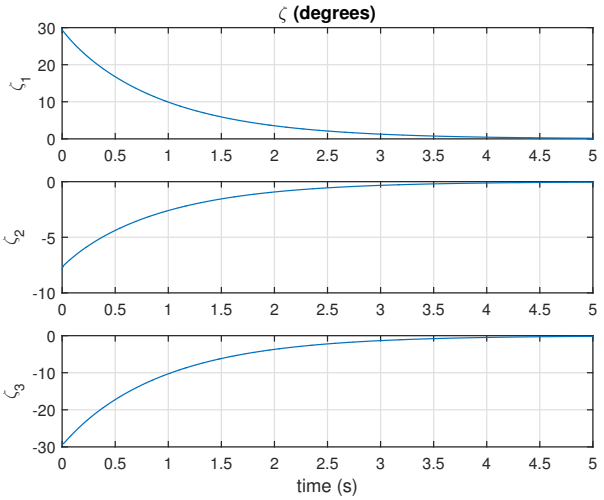

Fig. 8. Angle $\boldsymbol{\zeta}$ under inertia matrix perturbation, with compensation $\mathbf{u}$.

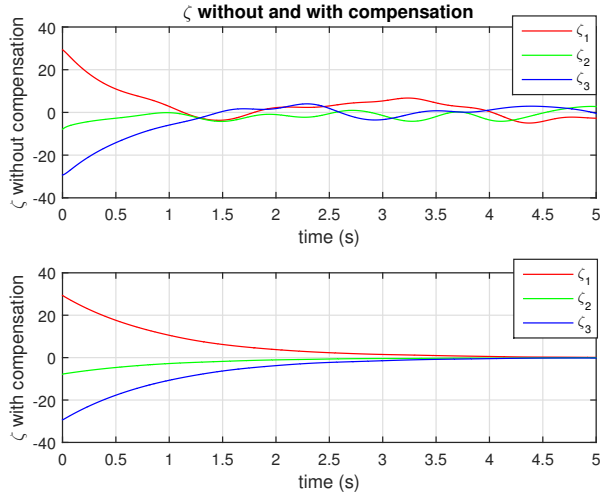

Fig. 9. Angle $\boldsymbol{\zeta}$ under the inertia matrix perturbation, the disturbance, and the compensation.

6) Fig. 9 shows the simulation under inertia matrix perturbation and random disturbance. The perturbation is given in (106). Here, for generality, the inertia matrix perturbation is nondiagonal. The value of δ_{tot} for the compensation (102) is $\delta_{tot} = \delta_1 + \delta_2 = 2.17 + 2 = 4.17$. The compensation reduces the bound of state variables and improves the system stability. In addition, the vibration (shown by the "wave" in the graph) is also reduced. This shows that the compensation in (102) can handle random disturbance and inertia matrix perturbation.

5.2. Discussion

The analysis is divided into 5 parts according to the number 1 to 6 in the Section 5.1. Note that the analysis of simulation no. 4 and 5 in Section 5.1 is combined in Subsection 5.2.4.

5.2.1 Nominal condition

The analysis of the simulation in nominal condition proceeds by using Theorem 1 and its proof. Based on equation (38) and using the numerical values, ε must be less than 0.0066; thus, we choose $\varepsilon = 0.005$. With this value, $\mathbf{P}_\varepsilon$ and $\mathbf{Q}_\varepsilon$ are positive definite matrices. Therefore, the closed-loop system is stable, as demonstrated by the simulation result in Fig. 3.

5.2.2 Chattering phenomenon

The chattering phenomenon is caused by the discontinuity of $\mathbf{u}$ when $\boldsymbol{\zeta}$ and $\boldsymbol{\Omega}_b$ equal zero. Therefore, the next simulations use small value of κ, i.e. $\kappa = 0.1$, which eliminates the discontinuity of $\mathbf{u}$ and the chattering in $d\boldsymbol{\Omega}_b/dt$. Chattering elimination is important to avoid large vibration, which may result in mechanical failure.

5.2.3 Under disturbance condition only

The simulation analysis in this subsection uses the Lyapunov analysis from Subsection 4.2.2. First, using the numerical values, let us calculate the values of c_{1I} to c_{4I}. They are

$$\begin{aligned} c_{1I} &= 0.0102, \\ c_{2I} &= 1, \\ c_{3I} &= 0.495, \\ c_{4I} &= 2.0001. \end{aligned} \tag{107}$$

Next, we must calculate the values of c_{1II} to c_{4II}. Before doing this, we have to determine $\mu_{\min}$. By taking $\boldsymbol{\zeta}_{\max} = \begin{bmatrix} \pi & \pi & \pi \end{bmatrix}^T$ and $\Omega_{b\max} = \begin{bmatrix} \pi/3 & \pi/3 & \pi/3 \end{bmatrix}^T$, and $\delta_1 = 2.17$, we get $\mu_{\min} = 0.0258$. Therefore, the values of c_{1II} to c_{4II} can be found as

$$\begin{aligned} c_{1II} &= 0.0102, \\ c_{2II} &= 1, \\ c_{3II} &= 3.01, \\ c_{4II} &= 2.0001. \end{aligned} \tag{108}$$

Let us calculate the bounds for both cases, i.e., b_I and b_{II}, in the following:

$$\begin{aligned} b_I &= \frac{c_{4I}}{c_{3I}} \sqrt{\frac{c_{2I}}{c_{1I}}} \frac{\Phi}{\Theta} = 39.97 \frac{\Phi}{\Theta}, \\ b_{II} &= \frac{c_{4II}}{c_{3II}} \sqrt{\frac{c_{2II}}{c_{1II}}} = 6.57 \frac{\Phi}{\Theta}. \end{aligned} \tag{109}$$

For fixed values of Φ and Θ, $b_{II} < b_I$. Therefore, if the disturbance compensation is introduced, the bound of state variables will reduce. This is justified by the simulation result in Fig. 6.

5.2.4 Under inertia matrix perturbation only

First, let us analyze the simulation under nondiagonal perturbation as given in (106). The perturbation matrix has 2-norm of $\|\Delta\mathbf{J}\| = 0.4$, which is smaller than the upper bound of $\|\Delta\mathbf{J}\|$, i.e., 0.61. According to equation (89), this perturbation can be handled by the compensation. Note that the values of $\Delta\mathbf{J}$'s elements are close to $\mathbf{J}_0$. Therefore, the compensation can handle the perturbation matrix whose elements are close to the elements of the nominal inertia matrix $\mathbf{J}_0$.

Next, we analyze the simulation under diagonal perturbation $\Delta\mathbf{J} = 0.5\mathbf{J}_0$, $\mathbf{K}_p = 8\mathbf{I}_{3\times3}$, and $\mathbf{K}_d = 5\mathbf{I}_{3\times3}$. The simulation demonstrates that the angle is stable and convergent toward zero. The analysis for this case proceeds using (98). Both $\mathbf{P}_\varepsilon$ and $\mathbf{Q}_\varepsilon$ can be made positive definite if ε is positive and its value is less than 0.0053; thus, the value of ε for this analysis is set to 0.005. With this, $\lambda_{\min}(\mathbf{Q}_\varepsilon)$ equals 0.62. The function $h(\|\boldsymbol{\zeta}\|, \|\boldsymbol{\Omega}_b\|)$ in (98) can have many values. In order to get the upper bound for $\|\Delta\mathbf{J}\|$, we seek the minimum value of $h(\|\boldsymbol{\zeta}\|, \|\boldsymbol{\Omega}_b\|)$. This is obtained by calculating the values of $h(\|\boldsymbol{\zeta}\|, \|\boldsymbol{\Omega}_b\|)$ for $\varepsilon = 0.005$ by entering the values of $\|\boldsymbol{\zeta}\|$ and $\|\boldsymbol{\Omega}_b\|$ from 0.00001 to $\pi\sqrt{3}$. After doing the numerical calculation by computation software, the minimum value of $h(\|\boldsymbol{\zeta}\|, \|\boldsymbol{\Omega}_b\|)$ is equal to 5.6. This is larger than the value of $\|\Delta\mathbf{J}\| = 0.5\|\mathbf{J}_0\|$, which is equal to 0.07. The upper bound $\|\Delta\mathbf{J}\| < 5.6$ is large. As comparison, $\|\mathbf{J}_0\|$ is equal to 0.1377. Therefore, if the disturbance is not present, the inertia matrix perturbation is diagonal, and $\mathbf{K}_p$ is diagonal with all of its elements are equal, the standard PD control in (21) can handle large inertia matrix perturbation.

5.2.5 Under inertia perturbation and disturbance

Fig. 9 shows that the compensation in (102) can handle the random disturbance and the inertia matrix perturbation, provided that δ_{tot} in (102) contains the contribution from the upper bound of random disturbance magnitude and $\Delta\mathbf{J}$.

6. CONCLUSION AND FUTURE WORK

In this paper, the design of disturbance compensation and its numerical testing are presented. The resulting control law consists of the nominal PD control law and the disturbance compensation term. The nominal PD control law can perform well in nominal condition. In order to counter random disturbance and inertia matrix perturbation, a disturbance compensation term is introduced. Chattering is avoided by avoiding discontinuity in disturbance compensation. The compensation term can reduce the effect of random disturbance, which is demonstrated by the decrease of state variable bound and the vibration. In addition, it can also counter the inertia matrix perturbation.

There is an interesting phenomenon if the disturbance does not occur, the inertia matrix perturbation is diagonal, and the proportional gain matrix is diagonal with equal elements. In this case, the PD control law without compensation can counter large inertia matrix perturbation.

Future work can be conducted to test the control algorithm in this paper with physical experiment using real quadrotor. In physical environment, the disturbance will be truly random. It will also be possible to investigate the implementation in computing hardware, such as microcontroller or single-board computer.

REFERENCES

[1] M. Elfeky, M. Elshafei, A. W. A. Saif, and M. F. Al-Malki, "Modeling and simulation of quadrotor UAV with tilting rotors," *International Journal of Control, Automation and Systems*, vol. 14, no.4, pp. 1047-1055, August 2016. [click]

[2] H. Lee and H. J. Kim, "Trajectory tracking control of multirotors from modelling to experiments: a survey," *International Journal of Control, Automation and Systems*, vol. 15, no.1, pp. 281-292, February 2017. [click]

[3] I. C. Dikmen, A. Arisoy, and H. Temeltas, "Attitude control of a quadrotor," *Proc. of 4th International Conference on Recent Advances in Space Technologies*, pp. 722-727, 2009.

[4] Y. Yu, "High performance full attitude control of a quadrotor on SO(3)," *Proc. of the IEEE International Conference on Robotics and Automation, 2015*, pp. 1698-1703, 2015. [click]

[5] T. Lee, "Global exponential attitude tracking controls on SO(3)", *IEEE Transactions on Automatic Control*, vol. 60, no. 10, pp. 2837-2842, October 2015. [click]

[6] Y. Yu, "Attitude tracking control of a quadrotor UAV in the exponential coordinates," *Journal of the Franklin Institute*, vol. 350, no. 8, pp. 2044-2068, October 2013.

[7] T. Lee, "Geometric tracking control of the attitude dynamics of a rigid body on SO(3)", *Proc. American Control Conference*, pp. 1200-1205, 2011.

[8] F. A. Goodarzi, D. Lee, and T. Lee, "Geometric control of a quadrotor UAV transporting a payload connected via flexible cable", *International Journal of Control, Automation and Systems*, vol. 13, no. 6, pp. 1486-1498, September 2015. [click]

[9] T. Lee, "Robust adaptive attitude tracking on SO(3) with an application to a quadrotor UAV". *IEEE Transactions on Control Systems Technology*, Vol. 21, No. 5, pp. 1924-1930, September 2013. [click]

[10] T. Fernando, J. Chandiramani, T. Lee, and H. Gutierrez, "Robust adaptive geometric tracking controls on SO(3) with an application to the attitude dynamics of a quadrotor UAV", *Proc. of 2011 50th IEEE Conference on Decision and Control and European Control Conference*, pp. 7380-7385, 2011. [click]

[11] K. Alexis, G. Nikolakopoulos, and A. Tzes, "Experimental constrained optimal attitude control of a quadrotor subject to wind disturbances," *International Journal of Control, Automation and Systems*, vol. 12, no.6, pp. 1289-1302, December 2014. [click]

[12] K. Alexis, G. Nikolakopoulos, and A. Tzes, "Experimental model predictive attitude tracking control of a quadrotor helicopter subject to wind-gusts," *Proc. of MED 2010*, pp. 1461-1466, 2010.

[13] S. Sheng and C. Sun. "An adaptive attitude tracking control approach for an unmanned helicopter with parametric uncertainties and measurement noises," *International Journal of Control, Automation and Systems*, vol. 14, no. 1, pp. 217-228, February 2016. [click]

[14] N. Sydney, B. Smyth, and D. A. Paley, "Dynamic control of autonomous quadrotor flight in an estimated wind field", *Proc. of 52nd IEEE Conference on Decision and Control*, pp. 3609-3616, 2013.

[15] N. K. Tran, E. Bulka, and M. Nahon, "Quadrotor control in a wind field", *Proc. of International Conference on Unmanned Aircraft Systems*, pp. 320-328, 2015.

[16] H. Huang, G. M. Hoffman, S. L. Waslander, and C. J. Tomlin, "Aerodynamics and control of autonomous quadrotor helicopters in aggressive maneuvering", *Proc. of the IEEE International Conference on Robotics and Automation, 2009*, pp. 3277-3282, 2009. [click]

[17] F. Bullo and R. M. Murray, "Proportional derivative (PD) control on the Euclidean group," *Proc. of 3rd European Control Conference*, pp. 1091-1097, 1995.

[18] R. M. Murray, Z. Li, and S. Sastry, *A Mathematical Introduction to Robotic Manipulation*, CRC Press, Boca Raton, 1994.

[19] A. Ataka, H. Tnunay, R. Inovan, M. Abdurrohman, H. Preastianto, A. I. Cahyadi, and Y. Yamamoto, "Controllability and observability analysis of the gain scheduling based linearization for UAV quadrotor," *Proc. of ROBIONETICS 2013*, pp. 212-218, 2013. [click]

[20] P. I. Corke, *Robotics, Vision and Control: Fundamental Algorithms in MATLAB*, Springer, Berlin, 2011.

[21] P. Pounds, R. Mahony, and P. Corke, "Modelling and control of a large quadrotor robot," *Control Engineering Practice*, vol. 18, no. 7, pp. 692-699, July 2010.

[22] D. Morin, *Introduction to Classical Mechanics: With Problems and Solutions*, Cambridge University Press, Cambridge, 2008.

[23] H. K. Khalil, *Nonlinear Systems*, Prentice Hall, Upper Saddle River, 2002.

Andreas P. Sandiwan obtained his bachelor degree Department of Electrical Engineering and Information Technology, Faculty of Engineering, Universitas Gadjah Mada, Indonesia. He started his undergraduate study in 2012, and finished it in 2016. His research interest involves control systems.

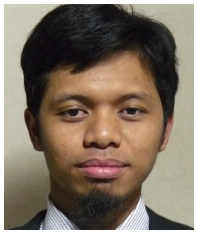

Adha Cahyadi obtained his bachelor degree from Department of Electrical Engineering (DEE), Faculty of Engineering, Universitas Gadjah Mada, Indonesia in 2002. Later he got his master in Control Engineering from KMITL in 2005, Thailand and Doctor of Engineering from Tokai University Japan in 2008. Currently he is serving DEE as the head of department. Dr. Cahyadi is an IEEE member. His research areas involves mechanical control systems, telemanipulation systems and unmanned aerial vehicles.

Samiadji Herdjunanto obtained his bachelor degree from Department of Electrical Engineering (DEE), Faculty of Engineering, Universitas Gadjah Mada (UGM). Later he got his master degree from Ohio State University, USA and doctoral degree from Universitas Gadjah Mada. Currently he is a faculty member of DEE UGM as associate professor. His research areas involves control, signal processing, fault detection, isolation and reconstruction.